# Petrographic signature of gravel fraction from late Quaternary glacigenic sediments in the Ross Sea (Antarctica): Implications for source terranes and Neogene glacial reconstructions

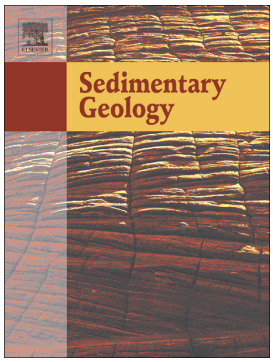


# Petrographic signature of gravel fraction from late Quaternary glacigenic sediments in the Ross Sea (Antarctica): Implications for source terranes and Neogene glacial reconstructions

Matteo Perotti, Luca Zurli, Kathy Licht, Gianluca Cornamusini

PII: S0037-0738(24)00165-9

DOI: https://doi.org/10.1016/j.sedgeo.2024.106742

Reference: SEDGEO 106742

To appear in: *Sedimentary Geology*

Received date: 14 June 2024

Revised date: 20 August 2024

Accepted date: 25 August 2024

Please cite this article as: M. Perotti, L. Zurli, K. Licht, et al., Petrographic signature of gravel fraction from late Quaternary glacigenic sediments in the Ross Sea (Antarctica): Implications for source terranes and Neogene glacial reconstructions, *Sedimentary Geology* (2024), https://doi.org/10.1016/j.sedgeo.2024.106742

# Petrographic signature of gravel fraction from late Quaternary glacigenic sediments in the Ross Sea (Antarctica): implications for source terranes and Neogene glacial reconstructions

Matteo Perotti [a], Luca Zurli [a,b], Kathy Licht [c], Gianluca Cornamusini [a,b]

[a] Department of Physical, Earth, and Environmental Sciences, University of Siena, Siena, Italy

[b] Museo Nazionale dell'Antartide – Siena Section, University of Siena, Siena, Italy

[c] Department of Earth and Environmental Sciences, Indiana University, Indianapolis, USA

*Corresponding author: matteo.perotti@unisi.it



## Abstract

The Ross Embayment is a key region to study the dynamics of the ice sheets during colder and warmer than present climatic conditions, because both the East and West Antarctic Ice sheets shed into the Ross Sea. Numerical modeling and reconstructions of the paleo ice flows during the Last Glacial Maximum show variable contribution of East and West Antarctic Ice sheets based on a variety of proxies.. In this study, we present the first petrographic and minero-chemical investigation of gravel-sized fraction of Last Glacial Maximum subglacial-glacimarine sediments collected with piston cores in a W-E transect across the Ross Sea. The clasts petrographic features are compared with outcropping geology to individuate the sediment source regions. The gravel content of the glacigenic diamictite was classified on the

basis of petrographic and minero-chemical features, and three main petrofacies were identified. They reflect changes in the basement geology of the source regions, allowing the reconstruction of paleo ice flow pattern and their comparison with scenarios built up with other datasets. Moreover, the comparison with the Oligocene to Pleistocene glacigenic sediments provided information about the changes of the gravel signature across the Ross Sea and the erosion history of the source regions during Cenozoic.

**Keywords:** provenance; diamictite; clast petrography; ice flows reconstruction; mineral chemistry

## 1. Introduction

The Ross Sea drains almost one third of the ice discharged from Antarctica (Anderson, 1999), thus it is a crucial area in understanding ice sheets dynamics over recent time. One of the most important aspects of this issue is to study the behavior of ice masses both from modern mass balance studies and from history of the Antarctic Ice Sheets in the recent past. Fronting this theme means also reconstructing the relative contribution of sectors of the Antarctic ice sheets that behave differently in terms of dynamics and climate control (Danielson and Bart, 2024 and reference therein). The partly marine-based West Antarctic Ice Sheet (WAIS) is particularly unstable and susceptible to ocean forcing (Mercer, 1978). Studies on the relative contribution of the WAIS and East Antarctic Ice Sheet (EAIS) in the Ross Sea during late Quaternary, in particular the Last Glacial Maximum (LGM), will help the construction of more reliable models able to describe also future behaviors of Antarctic Ice Sheet and its potential contribution to sea level rise (e.g., Deschamps et al., 2012; Pollard and DeConto, 2009). The knowledge of ice sheet history in the Ross Sea region has grown considerably during the past decades thanks to provenance studies on offshore and onshore glacigenic sediments using

different analytical approaches including mineral composition of the sand (Anderson et al., 1992; Hauptvogel and Passchier, 2012; Licht et al., 2005) and gravel fraction (Talarico et al., 2012; Perotti et al., 2018), geochronological and thermochronological studies (Licht and Palmer, 2013; Licht et al., 2014; Perotti et al., 2017; Li et al., 2020; Olivetti et al., 2023; Balestrieri et al., 2024) coupled with isotope geochemistry studies (Farmer et al., 2006; Farmer and Licht, 2016; Andrews and LeMasurier, 2021; Marschalek et al., 2021).

Several studies modeled the reconstruction and the dynamics of EAIS and WAIS during the LGM in the Ross Sea region (Denton and Hughes, 2000; Huybrechts, 2002; Pollard and DeConto, 2009; Golledge et al., 2012, 2013; Albrecht et al., 2020). Provenance analysis carried out on LGM tills by Licht et al. (2005, 2014), Farmer et al., (2006), Licht and Palmer (2013), demonstrated that EAIS and WAIS have had both a significant contribution in the LGM drainage pattern and that their flows converged in the Central Ross Sea at about 180° longitude. In particular, Licht and Palmer (2013) evidenced the role of the Byrd Glacier in discharging ice in the Western and central-western Ross Sea. In addition, some numerical models highlight the contribution of EAIS outlet glaciers discharge in the central Ross Sea (Golledge et al., 2012, 2013; Denton and Hughes, 2002), in comparison with sediment provenance data.

The aim of this work is to provide new data from gravel fraction to refine the existing provenance models and to propose a petrographic fingerprint of the Quaternary glacial sediments at a Ross Sea scale, extending the concept of “petrologic provinces” introduced by Anderson et al. (1984) over the gravel sized fraction. In addition, the in-depth study carried out is proposed as a present-day reference for evaluating the variability of gravel debris in

older sediments over the same geographic area to evaluate which lithologies act as a provenance marker and how they can vary through time (Licht and Hemming, 2017).

## 2. Physical and geological setting

The Ross Sea is bordered to the west by the Transantarctic Mountains (TAM) along the Victoria Land coast, to the east by Marie Byrd Land (MBL) in West Antarctica, to the south by the Ross Ice Shelf and to the north by the continental shelf break which deepens to the abyssal plain of the Pacific Ocean. The Ross Sea can be subdivided into three different regions: Western Ross Sea (WRS), Central Ross Sea (CRS) and Eastern Ross Sea (ERS) (Fig. 1).

The EAIS is terrestrial-based, primarily grounded on the continent above sea level. It is relatively slow flowing and diverging towards the coastlines (Anderson et al., 2002). As this ice crosses the Transantarctic Mountains , it accelerates through valleys via outlet glaciers. On the contrary, WAIS is mostly marine-based, grounded below sea level and characterized by regions of rapid flow and high discharge (Anderson et al., 2014). The greatest discharge of WAIS is provided by fast-moving ice streams converging in the Ross Sea along the Siple Coast. The Ross Ice Shelf (RIS) is constituted by ice discharged by the WAIS and the EAIS through the outlet glaciers of the southern Transantarctic Mountains . Paleo-troughs recognized in the Ross Sea floor are considered the erosive signatures of fast flowing ice during glacial maxima (Hughes, 1977).

The geology of the region around the Ross Sea is mainly known from rock outcrops along the Transantarctic Mountains to the west and south (e.g., Stump, 1995; Goodge, 2020; Talarico et al., 2022) and in Marie Byrd Land to the east (Jordan et al., 2020 and references therein;

Smellie et al., 2021). The geological features of the two macroregions are shown below in the next sections.

### 2.1. East Antarctica

The most extensive rock exposures are located along the Transantarctic Mountains that separate the EAIS and the WAIS (Fig. 1). These are formed of units spanning a period from Precambrian to Quaternary and are composed essentially by seven main groups of rocks. These are from the oldest to the youngest:

- Archean-Early Proterozoic Nimrod Complex and Argosy Schist (formerly the Nimrod Group) is an heterogeneous upper-amphibolite to lower granulite grade metamorphic complex. It is composed of banded quartzofeldspathic to mafic gneisses, schists, quartzites, marbles, as well as granitic to gabbroic orthogneisses, calc-silicate gneisses, relict eclogites and ultramafic pods (Goodge et al., 1993; Goodge and Mark Fanning, 1999; Goodge and Fanning, 2016; Stump, 1995; Goodge, 2020). The rocks of this group crop out mainly in the Miller and Geologists Ranges on the plateau side in the central Transantarctic Mountains (Stump, 1995; Goodge, 2020).
- Neoproterozoic metasedimentary and volcanic complexes related to rift margin deposition occurring in northern Victoria Land (portions of the Wilson Terrane rocks, Stump, 1995; Estrada et al., 2016), southern Victoria Land (Skelton Group; Gunn and Warren, 1962; Findlay et al., 1984; Stump, 1995; Cook and Craw, 2001, 2002), central and southern Transantarctic Mountains (Beardmore Group; Laird et al., 1971; Laird, 1991; Stump, 1995) and Pensacola Mountains (Patuxent and Hannah Ridge formations; Goodge, 2020). In general, these sequences are predominantly lower greenschist to upper

amphibolite grade rocks composed of greywackes, pelitic schists, quartzites, slates, paragneisses, and hornfelses (Laird et al., 1971; Laird, 1991; Stump, 1995; Goodge et al., 2002; Myrow et al., 2002; Goodge, 2020).

- Unconformably and tectonically overlying the Beardmore Group is the early-Cambrian Shackleton Limestone, cropping out between Beardmore and Byrd glaciers in the central Transantarctic Mountains, and which records a stage of platform carbonate deposition (Goodge, 2020). This unit is unconformably overlain by carbonate and siliciclastic rocks (Holyoake Formation, Douglas Conglomerate and Starshot Formation), which together define the Byrd Group (Stump, 1995; Myrow et al., 2002, Goodge, 2020). Siliciclastic units of the Byrd Group mark the termination of carbonate platform stage and the onset of molasse-type syn-orogenic deposition along the Gondwana margin, which also characterize other sectors such as northern Victoria Land with portion of Bowers, Wilson and Robertson Bay terranes (Goodge, 2020). In Queen Maud Mountains volcanic and volcanoclastic rocks are interbedded with carbonates and siliciclastic rocks (Rowell and Rees, 1989; Goodge, 2020); these Cambrian sequences (Wyatt, Ackerman, Taylor, Fairweather and Leverett Formations) are known as Liv Group (Stump, 1985; Rowell and Rees, 1989; Encarnación and Grunow, 1996; Rowell et al., 1997; Goodge, 2020) and are correlatives of the Byrd Group sequences in the central TAM.
- Cambrian-Ordovician Granite Harbour Intrusive Complex rocks are widespread as several plutons along the Transantarctic Mountains, cropping out from Ohio Range to northern Victoria Land (Stump, 1995). These are the result of a convergent plate margin setting and form a chiefly calc-alkaline magmatic belt along the Transantarctic Mountains (e.g., Goodge, 2020). These include a variety of foliated to isotropic biotite ± hornblende

granites, granodiorites to tonalites series, emplaced during the Ross Orogeny when the paleo-pacific plate subducted under East Antarctica. Late magmatism occurred at ca. 480 Ma (Allibone and Wysoczanski, 2002; Goodge, 2020).

- After the Ross Orogeny, exhumation of granitic and basement rocks produced the Kukri Erosion Surface (Barrett, 1991), an erosional unconformity that separates older rocks of East Antarctica from the Beacon Supergroup (Devonian to Jurassic). The Beacon Supergroup is mainly composed of fluvial sandstones, siltstones, conglomerates, shales, and coal measures (Barrett, 1991). It reaches a maximum thickness of 2.5-3.5 km and crops out from northern Victoria Land to the Ohio Range in the southern sector of the Transantarctic Mountains (Barrett, 1991).
- Intruding mainly Beacon Supergroup rocks, sills and dikes of the Jurassic Ferrar Group rocks including tholeiitic dolerite. Associated basalts and volcaniclastic rocks are also found throughout the region. These rocks are related to a rifting stage that occurred during the breakup of Gondwana and they are extended for 3500 km along the Transantarctic Mountains, with variable thickness ranging from 1 m to hundreds of meters (e.g., Elliot and Fleming, 2021).
- The McMurdo Volcanic Group (Cenozoic) is characterized by alkaline volcanic rocks ranging in composition from basalts to rhyolites, forming several outcrops, from small cones to large active volcanoes in a broad area comprising southern Victoria Land and portions of Western Ross Sea (Smellie and Martin, 2021; Smellie and Rocchi, 2021; Wilch et al., 2021; Geyer et al., 2023).

### 2.2. West Antarctica

Along the eastern margin of the Ross Sea, the best exposed rock units are located in Marie Byrd Land. The oldest unit cropping out in the Ford Ranges (Fig. 1) is the Neoproterozoic-Cambrian Swanson Formation, a sequence of sub-greenschist to greenschist siliciclastic rocks related to turbidite processes (Adams, 1986; Bradshaw et al., 1983; Pankhurst et al., 1998). This has been variably intruded during Devonian-Carboniferous and Cretaceous times by the I-type Ford Granodiorite suite and the A-type Byrd Coast Granite suite, respectively, with episodes of migmatization and high-grade metamorphic events, recorded for example in the Fosdick Mountains (Siddoway et al., 2004). The emplacement of the youngest components of Byrd Coast Granite coincides with the onset of regional extension to transtension and the development of the West Antarctic Rift System (Siddoway, 2008; Jordan et al., 2020). Pre-Cenozoic rocks in Marie Byrd Land are marked by an erosive surface, the West Antarctic Erosion Surface (LeMasurier and Landis, 1996), while during the Cenozoic, the region was affected by intense alkaline volcanism and uplift of a volcano-tectonic dome. This activity started at about 34 Ma (Rocchi et al., 2006), followed by initial uplift of the dome around 28-30 Ma. Eighteen major shield volcanoes and many smaller centers are known from the region, composed of felsic alkaline lavas, even if these felsic varieties are supposed to build up <10% of the total volcanic rocks in the province (LeMasurier et al., 2011).

## 3. Materials and Methods

### 3.1. Sampling strategy

A total of 42 piston cores collected by different scientific cruises across the Ross Sea were logged and sampled at the Marine Geology Antarctic Research Facility of Tallahassee, Florida (Fig. 1 and Table 1). Seventeen of 42 cores have been already studied by Perotti et

al. (2017). For some cores (i.e., cores 80-133 and 80-189 in WRS and 94-36, 95-11, 95-17 in the CRS), detailed stratigraphic and chronological analysis were available in the literature (Licht and Andrews, 2002; McKay et al., 2008; Licht et al., 1999).

Logging was completed to identify the composition of the gravel fraction (i.e. granule to cobble sized clasts) along the intervals of each core representing proximal glacimarine and subglacial till facies, considered to be directly related with glacial transport. The size, shape and features of each clast >2 mm was determined for each 10 cm interval of the working half split surface of the core, following the same procedures applied in Talarico and Sandroni (2009). Based on distinctive macroscopic properties, clasts were grouped into six major lithological groups (volcanic rocks, intrusive rocks (except dolerite), metamorphic rocks, sedimentary rocks, quartz fragments, and dolerite). Dolerite was highlighted separately from other igneous rocks because of its distinctly East Antarctic provenance. A summation of all clasts from different lithological groups was carried out for each core. Table 1 also shows the number of logged clasts for each half-split surface of cores. A total of 2187 clasts were counted, measured and classified from the 42 cores, and from these 345 representative clasts (pebble to cobble sized) were sampled for detailed petrographic analysis.



### 3.2. Petrography

#### 3.2.1. Analytical Details

A selection of 38 representative pebble sized clast thin sections was examined under a polarized microscope in order to establish a detailed mineralogical and textural analysis for each sample. These are a selection from Central Ross Sea (CRS) and Western Ross Sea (WRS), while representative samples from Eastern Ross Sea (ERS) are described in Perotti

et al. (2017). The identification of possible source rocks for pebbles was carried out thanks to a representative collection of rocks stored at the National Antarctic Museum of Siena – Italy (https://www.mna.it/) and The Polar Rock Repository (PRR), Byrd Polar and Climate Research Center (BPCRC), Ohio State University.

### 3.2.2. Mineral Chemistry

Mineral chemistry analysis was carried out on 8 representative clasts. These are hornblende-tonalite (thin section 24), three biotite-white mica schists (thin section 25, 35 and 83), biotite-amphibole schist (thin section 26), two metasandstones (thin section 92 and 95) from CRS cores and an intermediate alkaline basalt from WRS (thin section 71). They were chosen on the basis of the presence of unaltered minerals on their surfaces. Chemical analysis of the main mineral phases identified via petrographic microscope was carried out with an X-ray energy dispersive system EDAX DX4 attached to a Scansion Electron Microscope Philips XL30 at the Department of Physical Sciences, Earth and Environment of Siena (Italy). Thin sections were polished and carbon coated before carrying out measurements. Analytical conditions were 20 kV of accelerating voltage, 25 µA of emission current, 0.1 nA beam current and a beam spot size of 0.2 µm. Natural minerals were used as standards. $Fe^{3+}$ concentration in clinoamphiboles was estimated by the equation of Droop (1987), assuming charge balance.

## 4. Results

### 4.1. Petrographic results and clasts distribution

This section describes the main petrographic features of the samples collected from the analyzed sediments, followed by distribution of different lithotypes across the Ross Sea region. Petrographic features and distribution of ERS samples are shown in Perotti et al. (2017), while clasts recovered from CRS and WRS piston cores are described as follows and shown in Table 2. Granodiorite to tonalite clasts are gray to pinkish inequigranular, sometimes porphyritic, fine to medium grained with hypidiomorphic texture (Fig. 2A). They include biotite ± green hornblende as mafic minerals and apatite, zircon and titanite as accessory phases. In another case (thin section 24; Fig. 2A) epidote is associated with clinoamphibole. Quartz sometimes forms a granophyric interstitial texture with k-feldspar (thin section 32). Leucocratic syeno-granite has an hypidiomorphic to allotriomorphic, equigranular medium grained texture with minor plagioclase, perthitic orthoclase and quartz (Fig. 2C). Mafic varieties include medium-grained sub-ophitic gabbro, constituted by brownish clinopyroxene, plagioclase, opaque minerals, and interstitial minor quartz with granophyric texture.

Sub-volcanic rocks include dolerites (Fig. 2B), characterized by a fine grained sub-ophitic texture defined by clinopyroxene and plagioclase, with minor opaque minerals. Sometimes quartz is present as a minor interstitial phase.

Volcanic rocks include two rhyolitic samples (Fig. 2D-F), characterized by medium grained phenocrystals of quartz and minor plagioclase set in a very fine-grained quartz-feldspar groundmass. In one of these samples (thin section 36; Fig. 2F) groundmass is recrystallized with neoblastic tiny biotite. A sample of intermediate lava (thin section 71; Fig. 2E) shows an ipocrystalline texture with medium grained phenocrystals of zoned augite and brown amphibole, set in groundmass rich in plagioclase, clinopyroxene, minor sanidine and abundant glass.

Metamorphic rocks are generally characterized by fine to medium grained isotropic to grano-lepidoblastic textures and they show typical paragenesis suggesting a sedimentary (pelitic-psammitic) origin of the protoliths (Fig. 3). They include biotite ± white mica fine grained schists, in which foliation is defined by isorientation of tiny biotite idioblasts, alternating to granoblastic quartz-plagioclase domains (Fig. 3E-F). Metasandstones include fine to medium/coarse grained, weakly to moderately foliated rocks that preserve the original clastic texture, with quartz, feldspars and lithic grains, more or less enveloped by tiny biotite idioblasts to xenoblasts, which sometimes define a weak foliation (Fig. 3G). In weakly foliated varieties, epidote xenoblasts are also present. Fine grained phyllites include a sample defined by orientation of biotite, calcite, and quartz, with poikiloblastic medium grained pale green actinolite (thin section 37; Fig. 3I). A sample of medium grained marble is characterized by a polygonal weakly foliated texture of calcite and rare opaque minerals (thin section 94; Fig. 3H).

Sedimentary rocks are fine to coarse grained, poorly sorted, heterogranular siltstone to sandstones, with variable amount of matrix (Fig. 3C-D). Moreover two samples of carbonate rocks have been examined: one sample (thin section 33; Fig. 3A) of very fine grained microsparitic limestone, with stylolites and few areas of recrystallized calcite; and one sample (thin section 91; Fig. 3B) of recrystallized microsparitic limestone with a mosaic texture of fine-grained calcite crystals. In addition to extrabasinal sedimentary clasts, a certain amount of intrabasinal clasts were found from the analyzed cores: these are polymictic fine- to coarse-grained matrix-rich non-consolidated soft sediments incorporating lithics grains and quartz crystals; in some case they have granule grain size, in others they are silt-size.

Gravel clasts from CRS cores have an overall similar composition of those found in ERS (see Perotti et al. 2017 for further details)Metamorphic (low-grade) lithic clasts are the most common lithology, ranging from 20% to 94%, followed by granitoids (4-49%) and sedimentary lithics (0-67%), while dolerite and volcanic lithics are negligible. Putting all the CRS cores together, the average proportion of lithologies is as follows: metamorphic lithics 64.9%, granitoids 18.3%, sedimentary clasts 9.9%, quartz 5.5%, dolerite and volcanic lithics below 1%.

Western Ross Sea cores are characterized by a distinct, although variable, clast assemblage. Indeed, in 3 out of 9 cores (i.e. 80-189; 78-09; 94-16), volcanic rock fragments compose the major fraction of clasts assemblage, up to 69% of the total for the core 78-09. The cores richest in volcanic clasts are primarily located close to Ross Island in McMurdo Sound. The exceptions are cores 32-13 and 94-16, which have a volcanic percentage of 35% and 64% respectively, and are located in the Joides Basin, nearly 200 km offshore from Ross Island (Fig. 1). The second most represented lithology is the group of metamorphic rocks, composed of mainly low-grade isotropic to slightly anisotropic fine to medium-grained metasandstones, siltstones, and quartzites. This group has an average occurrence of 45% among the WRS cores. Granitoid lithic fragments are present in variable amounts and they range from 0% to 44%. Sedimentary clasts are prevalently matrix-rich sandstone and siltstone in minor proportion, except in one core (i.e. 94-02) where they reach 39% of the total clast assemblage. Considering all the counted clasts together as a single group, WRS cores have an overall composition consisting of a major fraction of volcanic rock fragments (35.1%) and metamorphic rocks (38.4%), followed by granitoids (8.6%), and sedimentary rocks (14.1%).

Looking at the spatial distribution of analyzed cores and taking into account their positions, the main differences in clast distribution between ERS, CRS, and WRS cores is the amount of 1) volcanic lithologies (WRS = 35%, <1% CRS and ERS), 2) Granitoid rock fragments (CRS = 18%, ERS = 10.6% and WRS = 8.6%,), and 3) metamorphic rock fragments ERS = 72.2%, CRS = 64.9%, WRS = 38.4%). Figure 4 shows clast occurrence and distribution from analyzed cores along an ideal transect spanning from Marie Byrd Land to Southern Victoria Land coast.

The following broad lithological associations of clasts (i.e., petrofacies) are proposed on the basis of collected data (Fig. 5). Discriminant analysis was carried out to validate the association of core to specific petrofacies, and to verify that the three clusters do not overlap (Fig. 5).

- Petrofacies A: it comprises fine-grained metamorphic rocks such as phyllite, meta-sandstone, biotite ± white mica schist, quartzite, and they are associated with biotite ± hornblende granodiorite to tonalite. In this assemblage, granitoids are very minor compared to metamorphic rocks, which constitute at least 55% of the total clast assemblage. Volcanic rocks are always < 20% of the total.
- Petrofacies B: it comprises > 20% basalt and intermediate volcanic rocks. Low-grade metamorphic rocks, such phyllite, pelitic schist, and meta-sandstone, are more common than biotite ± hornblende granodiorite to tonalite.
- Petrofacies C: it comprises the same lithologies described for the other petrofacies, but in this case the amount of granitoid lithics exceeds 30% of the total.

### 4.2. Mineral Chemistry

Clinoamphiboles were analyzed from three thin sections (24, 26, 71). All analyzed amphiboles are members of the calcic-amphibole group, as shown in Figure 6A (Leake et al., 1997). Clinoamphiboles in biotite amphibole schist (thin section 26) are magnesio-hornblende to actinolites in composition, with $X_{Mg}$ of the cores varying from 0.63 to 0.77, and they are mostly slightly zoned, with a Mg-richer core and a Fe-richer rim. In biotite-amphibole tonalite (thin section 24), amphiboles are mostly magnesio-hornblendes to actinolitic hornblendes ($X_{Mg}$ ranging from 0.51 to 0.64), in some cases having a strong zonation, with Fe-richer rim and Mg-richer core. In alkaline basalt (thin section 71) amphiboles phenocrystals belongs to the pargasite-edenite series ($X_{Mg}$ ranging from 0.62 to 0.68), and they have Ti>0.50 atoms per formula unit, so they are all kaersutites, according to Leake et al. (1997) classification.

In most samples (e.g. thin section 83), biotites have a narrow compositional range ($X_{Fe}$ 0.46-0.48), and quite homogeneous composition. Biotite from thin section 35 exhibits in some cases strong zonation, with Fe enrichment and Mg depletion from core to rim. In general, all the analyzed biotites have $X_{Fe}$ between 0.46 (thin section 83) and 0.64 (thin section 35), with variable amounts of $Al^{IV}$ (Fig. 6B).

White micas in petrographically similar metasandstones (thin sections 92 and 95), biotite schist (thin section 83) and biotite-white mica ± garnet schist (thin section 35) are all muscovites; in certain cases they exhibit a wide range of composition, for example in thin section 92 and to a lesser extent in thin section 95 and 35, some single idioblasts have a more phengitic composition, even if the majority of idioblasts have an average amount of Si per formula unit <6.3 (Fig. 6C). Instead, another biotite-white mica schist (thin section 25) has an average composition richer in Si per formula unit, ranging between 6.3 and 6.5.

## 5. Discussion

The petrographic distribution of gravel sized clasts reveals differences that can be grouped into three petrofacies. This gravel detritus suggests that ice is transporting lithologically distinct bedrock around Ross embayment. The implications of the present study are discussed here in terms of i) source rocks capable of producing the detritus found in the Quaternary sediments; ii) identification of distinct petrographic provinces and implications for source terranes; iii) Variability of the gravel composition and identification of lithologies able to mark shifts in ice sheet dynamics in recent and older sediments.

### 5.1. Clasts source rocks from outcropping geology

The majority of analyzed clasts are low-grade fine- to medium-grained metasedimentary rocks. They show sub-greenschist/greenschist grade paragenesis, with occurrence of biotite ± chlorite ± (garnet) ± white mica in metasedimentary rocks. Calcite ± epidote ± white mica assemblages are present in more Ca-rich rocks. In some cases, foliation is not clearly developed and only a static recrystallization occurs, with growth of biotite or actinolite porphyroblasts. Moreover, also mineral chemistry analysis of micas (fig. 6), even if data are scattered, suggest a thermo-metamorphic regime referable to low/medium grade conditions and are comparable to similar lithologies found in the same region from coeval and older sediments (Perotti et al. 2017; Zurli et al. 2022). These features are useful to identify potential sources from low-grade metamorphic units, which also experienced a thermal overprinting caused by pluton emplacement. Table 1S shows all possible source units for each type of rocks identified in thin section, with a subdivision between eastern sources (i.e. Transantarctic Mountains) and western sources (West Antarctica-Marie Byrd Land).

Meta-sandstones, meta-siltstones, phyllites (sometimes with spotted thermometamorphic overprint), quartzites, and bt-schists are present in (meta)sedimentary units in several areas in the Transantarctic Mountains. Starting from southern Victoria Land, rocks of regional metamorphism with low P-T conditions occur in the Skelton-Mulock glaciers region (Skinner, 1982; Cook and Craw, 2002; Cox et al., 2012). Farther South, in the central Transantarctic Mountains around Nimrod Glacier, a sequence of thermally metamorphosed greywacke and shales is part of the outboard Goldie Formation, correlative of the younger Starshot Formation of the Byrd Group (Laird et al., 1971; Stump, 1986, 1995; Myrow et al., 2002; Goodge et al., 2002). The regional metamorphism and the paragenesis of Byrd Group rocks are typical of a low P/T assemblage (Skinner, 1965), except for a restricted area in the south side of the Byrd Glacier (Selborne Marble, Stump et al., 2004; Talarico et al., 2007). Other outboard sequences temporally correlatives with the Cambrian Byrd Group are located farther South, in the Queen Maud Mountains (Stump, 1986, 1995). In particular the La Gorce, Duncan, and Party formations, which include meta-greywackes, siltstones, quartzites, and schists cropping out between the Scott and Reedy glaciers area, and interpreted as deposits related to turbidity currents processes (Stump, 1981, 1986, 1995). Even if meta-sedimentary rocks locally occur where the Beacon Supergroup experienced conditions of contact metamorphism (Barrett, 1966; Balance and Waiters, 2002; Bernet and Gaupp, 2005), this cannot be considered a reliable source of low-grade meta-sedimentary rocks due to different petrographic and textural features of the Beacon's rocks and the scarcity of unmetamorphosed Beacon clasts.

The only known potential sources of metasedimentary rocks in West Antarctica is the Cambrian-Ordovician Swanson Formation, which crops out mainly in Ford Ranges in western

Marie Byrd Land. This formation has been correlated chronologically within the Robertson Bay Group in northern Victoria Land (Bradshaw et al., 1983; Adams et al., 2013; Pankhurst et al., 1998), and correlative metasediments are exposed in scattered isolated nunataks in the region of Eastern Marie Byrd Land (Hobbs Coast and Ruppert Coast; Brand, 1979; Pankhurst et al., 1998).

Marbles are present in several regions of the Transantarctic Mountains. In southern Victoria Land they occur as a minor component in the Skelton Group between Blue and Koettlitz glaciers (Findlay et al., 1984), and in the region of the Skelton Glacier (Cook and Craw, 2002). In the central Transantarctic Mountains, marble crops out along the southern side of Byrd Glacier (Selborne Marble; Skinner, 1964, 1965). Impure limestones and marbles are subordinately interbedded in the Cobham and Goldie formations of the Beardmore Group (Laird et al., 1971; Myrow et al., 2002; Stump, 1995). In the Miller and Geologists Ranges, the Nimrod Complex and Argosy Schist contain calc-silicates and subordinate tremolite-bearing marbles (Stump, 1995; Goodge 2020). Limestone of the Shackleton Limestone Formation of the Byrd Group crops out in the region between Byrd and Nimrod glaciers (Laird et al., 1971; Myrow et al., 2002). In the Queen Maud Mountains, marbles and limestones have been identified in outcrops of Taylor Formation, in the Shackleton Glacier region, while marbles occur also in the Fairweather and Henson Marble Formations in the Liv Glacier area (Stump, 1986, 1995). Marble- and limestone-bearing units are absent from the Ross Sea catchment in West Antarctica (marble outcrops are in eastern Marie Byrd Land at Mt Murphy, and limestones in the Ellsworth-Thiel and Pensacola mountains, Stump, 1995; Pankhurst et al. 1998), but the most likely source rocks of carbonate clasts to the Ross Sea are located along the Transantarctic Mountains. A younger possible source of carbonate rocks are the

calcareous sandstones and limestones as revealed from the Eocene McMurdo erratics (Levy and Harwood, 2000) probably occurring in the Discovery Deep below the Ross Ice Shelf at the front of the Transantarctic Mountains (Paulsen et al., 2011; Talarico et al., 2013; Cornamusini and Talarico, 2016).

Igneous rocks found in the marine dataset are prevalently biotite ± hornblende granodiorite to tonalite, but a sample of biotite monzogranite, a sample of syeno-granite and two samples of gabbros are also present. The source of granitoid rocks in Ross Sea cores is ambiguous because of their prevalence in both East and West Antarctica. In Marie Byrd Land, granodiorites and hornblende-tonalites are the main lithologic types of the Devonian-Carboniferous Ford Granodiorite (Weaver et al., 1991; Pankhurst et al., 1998), whereas syeno-granites are more common types in the Cretaceous alkaline Byrd Coast Granite suite (Weaver et al., 1992). Along the Transantarctic Mountains, in southern Victoria Land hornblende-bearing granodiorite isotropic to strongly heterogranular monzogranite plutons crop out extensively (Gunn and Warren, 1962; Simpson and Cooper, 2002; Cox et al., 2012). Tonalites are instead more represented in the Blue Glacier area, while syenogranites are present as part of the Koettlitz Glacier Alkaline Suite which crops out mainly at the head of Koettlitz Glacier (Read et al., 2002; Cox et al., 2012). South of the Byrd Glacier discontinuity, granitoids are less extensive and represented by muscovite ± hornblende quartz-monzonites and granites of the Hope Granite (Laird et al., 1971; Stump, 1995); tonalites are also reported at the head of Nimrod Glacier (Laird et al., 1971; Stump, 1995). In the Queen Maud Mountains, the Granite Harbour Intrusive Complex is mainly represented by the Queen Maud-Wisconsin Range Batholith (Stump, 1995), composed of granite and quartz-monzonite to

tonalite, diorite and hornblende gabbro, with medium- to coarse-grained, equigranular and porphyritic granodiorites-quartz monzonites, containing biotite and locally hornblende.

Along the Transantarctic Mountains, gabbro is limited to small intrusions in the Granite Harbour Intrusive Complex (Simpson and Aslund, 1996; Cox et al., 2012; Read et al., 2002; Cottle and Cooper, 2006b; Stump, 1995); gabbro and dolerite are the main lithologies of the Ferrar Group that largely crops out along the Transantarctic Mountains (Elliot and Fleming, 2021 and reference therein). However, these types of rocks are present also in central Marie Byrd Land in West Antarctica in the form of mafic dykes and small intrusions, relating to the Cretaceous rifting phase of the West Antarctic Rift System (Weaver et al., 1994; Storey et al., 1999; Saito et al., 2013). Thus, an absolute attribution of detrital gabbros and dolerites to the Ferrar Group of the Transantarctic Mountains is not possible, however this is the most likely source based on their widespread spatial extent.

Sedimentary clasts in the marine dataset, comprise heterogranular, moderately sorted, matrix-rich sub-arkoses, sandstones, and siltstones that most likely derive from Beacon Supergroup sequences, which are exposed in the interior of the Transantarctic Mountains. Usually, at least in southern Victoria Land, arkose and litharenite are characteristic of the Victoria Group, whereas quartzarenites and sub-arkoses are more typical of the underlying Taylor Group (Cornamusini and Talarico, 2016; Cornamusini et al., 2023; Zurli et al., 2024a). In one case, a coarse-grained sandstone clast (thin section 29) containing lithic fragments of different lithologies (plutonic, quartzites, low grade metamorphic lithics, and carbonates) could be possibly considered as intrabasinal clast, even if its petrographic characteristics, except for its lack of fossils, are similar to those of the McMurdo Erratics (Levy and Harwood, 2000) sourced from the Discovery Deep (Paulsen et al., 2011). Sedimentary bedrock is not exposed

in Marie Byrd Land, however, sedimentary sequences, unmetamorphosed equivalents of the Swanson Formation, are thought to exist beneath WAIS in the inner region of the Ford Ranges and Edward VII Peninsula (Luyendyk et al., 2003).

Mafic volcanic clasts have been prevalently found in WRS, adjacent to the McMurdo Volcanic Group outcrops from volcanic islands and peninsulas in McMurdo Sound (Ross, Black, White islands, Minna Bluff). Basic and intermediate detrital lithotypes (e.g. thin section 71 and 74) could be confidently related to the McMurdo Volcanic Group rocks. Mineral chemistry analyses carried out on thin section 71 revealed presence of brown kaersutite amphibole (Figure 5), which is typical of the intermediate lavas of the Erebus Volcanic Province (Smellie and Martin, 2021). Felsic varieties have a less distinctive provenance. Rhyolites are minor component in the Erebus Volcanic Province (Martin et al., 2010). Rhyolites are also intercalated with metasedimentary rocks in the Liv Group in the Queen Maud Mountains (Stump, 1986, 1995; Rowell and Rees, 1989, Goodge 2020), or they occur as clast in the Beacon Supergroup (Wysoczanski et al. 2003; Zurli et al. 2024b). In West Antarctica, volcanoes located in Marie Byrd Land are rich in felsic varieties such as pantellerite and pantelleritic trachytes rocks, with minor rhyolites (LeMasurier et al., 2011; Wilch et al. 2021).

### 5.2. Petrographic provinces for late Quaternary glaciomarine sediments

Petrofacies distribution along an ideal W-E transect in the Ross Sea mirrors the relative contribution of eroded lithologies from both sides of the Ross embayment. Cores subdivided following the PF classification are shown in Figure 7. The latter clearly shows that Petrofacies A is the most widespread and it is present in ERS, CRS and WRS cores. As a whole, the PF-A suggests a possible source region defined by a low P/T meta-sedimentary terrain, locally

intruded by plutons. This geological setting is present in Marie Byrd Land and in different locations in the Transantarctic Mountains front as well, for example in the Skelton-Mulock glaciers area (Cook and Craw, 2002; Cottle and Cooper, 2006a), or in the Central Transantarctic Mountains south of Byrd Glacier discontinuity (Stump, 1995; Goodge et al., 2002; Goodge 2020). Thus, the Petrofacies A alone is not sufficient to discriminate a clear lithologic signature from the Transantarctic Mountains or from West Antarctica (Table 3).

Minor but diagnostic lithologies could indicate provenance from East Antarctica. For example, one possible source region for carbonates is represented by the central Transantarctic Mountains sector, from the Byrd to the Beardmore glaciers (Table 3). Previous provenance studies demonstrated that ice fed by Byrd Glacier during the LGM has its easternmost extension over site 27-14 in CRS (Licht and Palmer, 2013). East of this site in CRS, geochronologic and petrographic data suggest a mixing process between ice fed by Byrd Glacier and that fed by Nimrod Glacier, the latter becoming more relevant to the east and indicated by a sand-sized oolitic limestone grain (Licht et al., 2005; Licht and Palmer, 2013; Farmer and Licht, 2016). This is coherent with clasts dataset, with limestone and marble clasts, that could be sourced from carbonate sequences of the Byrd Group (e.g., Shackleton Limestone), low-grade metasedimentary clasts sourced from the Beardmore and Byrd groups sequences, sedimentary extrabasinal siliciclastic clasts sourced from Beacon Supergroup rocks, and minor dolerite clasts sourced from Ferrar Supergroup rocks. Looking at the geomorphological features in the Ross Sea floor (Halberstadt et al., 2016), the Glomar Challenge Basin shows lineation directions that could be compatible with ice flows from the Byrd and Nimrod glaciers, supporting the occurrence of carbonate clasts in the basin (Fig. 7). The occurrence of rare carbonate (i.e., core 78-12) clasts east of the westward core with

Cretaceous U/Pb signature indicating a provenance from West Antarctica (Licht et al., 2014) could have different explanations: i) the Glomar Challenge Basin recorded a mixing of West Antarctica and Transantarctic Mountains ice flows; ii) the carbonates were reworked from older sediments deposited in different ice flow pathway; iii) the ice flow trajectories changed during the LGM as, in a model referable to the "dynamic flow-switching scenario" of Halberstadt et al. (2016).

In some cases, minor but potentially distinctive lithologies have a less clear provenance. Felsic (meta-) porphyries, associated with low-grade sedimentary clasts, are lacking in the Petrofacies A, suggesting that Queen Maud Mountains (QMM) terrane may represent a minor source area, since most of the basement rocks in QMM are the interbedded (meta-)volcanic and (meta-)sedimentary units of the Liv Group (Stump, 1985; Rowell and Rees, 1989, Goodge 2020). However, a contribution from outlet glaciers of QMM (e.g., Scott and Reedy Glaciers) to the CRS sediments could not be excluded *a priori*, since rhyolitic porphyries clasts rarely occur and they could suggest a dismantling of Liv Group. However, a possible source of the felsic porphyritic rocks are the Cenozoic volcanic edifices in West Antarctica (Wilch et al., 2021 and reference therein) .

Petrofacies B cores are all located in the WRS and in some cases, distal to the volcanic islands of McMurdo Sound (i.e., cores 32-13, 94-16, 94-12) (Fig. 7). These cores are rich in volcanic detritus likely derived from the McMurdo Volcanic Group, and their distribution is limited to the Central and Joides basins (Table 3). The boundaries for Petrofacies B are constrained by ice flow reconstructions based on combined sediment provenance data and linear sub-glacial geomorphic features (Shipp et al., 1999; Licht and Palmer, 2013; Anderson et al., 2014; Halberstadt et al., 2016). Distribution of volcanic clasts is coherent with a

scenario of ice flowing northward divided by the Ross Bank, as documented by glacial lineations on the seafloor (Shipp et al., 1999; Halberstadt et al., 2016). The portion of ice that flowed west of the Ross Bank into the Central and Joides basins must have carried out volcanic detritus after its passage around Ross Island, while the portion flowing eastward did not erode any volcanic source rock; this is indirectly evidenced by the absence of Petrofacies B cores east of Ross Bank and emphasizes the role of a major geomorphic ice-divide. In WRS, clasts dataset reflects the importance of McMurdo Volcanic Group detritus associated to low-grade metasediments and granitoids: this points out to an important flux of ice discharged by Mulock and Skelton glaciers able to erode McMurdo Volcanic rocks and to leave their detritus over distal positions as the Joides Basin (i.e. sites 32-13, 94-16, 94-12). Metasediments found in WRS cores are petrographically similar to those found in ANDRILL sites and interpreted to be sourced in Skelton Mulock-Glacier region (Talarico and Sandroni, 2011; Sandroni and Talarico, 2011). Moreover, any clast association has been found in analyzed cores revealing higher pressure conditions and medium/high-grade metamorphic regime, which is localized in Britannia Range, between Darwin and Byrd glaciers (Carosi et al., 2007). However, since it has been demonstrated that ice discharged by Darwin and Byrd glaciers has an important draining role in WRS during glacial maxima (Talarico and Sandroni, 2011, Licht and Palmer, 2013, McKay et al., 2016), it is possible that WRS analyzed cores reflect a mixed contribution from both Skelton-Mulock glaciers area and Darwin-Byrd glaciers region, since some Holocene sites ca.60 km east of Ross Island have yielded detrital clasts from Darwin and Byrd glaciers region (McKay et al., 2016).

It is remarkable that only few and scattered volcanic pebbles have been found from CRS and ERS cores, despite the hypothetical occurrence of large volumes of volcanic rocks in the

West Antarctic Rift System beneath the ice (Van Wyk de Vries et al., 2018). These large volumes of rocks should provide some detrital trace in offshore deposits useful for tracing ice stream dynamics. Instead, our findings shows that volcanic pebbles are largely a minority, in agreement with what is found in by sand fraction (Licht et al., 2005), by Vogel et al. (2006) in West Antarctica subglacial sediments and, more recently, by Andrews and LeMasurier (2021) in offshore sediments collected in front of the Ross Ice Shelf. In general, the more mafic fingerprint, defined by abundance of pyroxenes, olivines, basaltic, and doleritic lithic grains of WRS sediments compared to those from the CRS and ERS is confirmed by our dataset. The paucity of volcanic clasts in the Ross Sea sediments lead to questions about the occurrence of subglacial volcanoes beneath the ice sheet within the West Antarctic Rift System, which could act as drivers for melting of the WAIS. Vogel et al. (2006) and Andrews and LeMasurier (2017) hypothesized the absence of large late Cenozoic volcanic provinces in the interior West Antarctic Rift System, also corroborated by the thermal gradient values that does not support active volcanism (Winberry and Anandakrishnan 2004). Recent geochronological investigations on sand size fraction from the Byrd Ice Core revealed the occurrence of a small proportion of Miocene to recent volcanic hornblende, pointing out a limited Late Cenozoic volcanism beneath the West Antarctic Rift System (Marschalek et al., 2024). Miocene sediments in the CRS, with inferred West Antarctica provenance, have basaltic clasts (Marschalek et al., 2021; Zurli et al., 2022), while Balestrieri et al. (2024) recorded Oligocene detrital apatites from DSDP Site 272 in the CRS. Those data support the volcanic activity at least in Oligocene-Miocene in West Antarctica sectors. Therefore, it could be speculated that volcanism was active in the Neogene but that volcanic products are largelyunavailable in the Quaternary due to erosion or burial of volcanic centers or changes in the ice flow pathways.

Petrofacies C is characterized by similar lithologies occurring in PF-A, but with different relative proportions; granitoid lithics are more abundant in PF-C than PF-A. Cores showing PF-C assemblage are located in the CRS and ERS regions. Detrital data from the sand fraction of comparable sediments show an increase of quartz-feldspar and felsic intrusive lithic fragments in the ERS region, together with a decrease of mafic minerals and lithic grains (Licht et al., 2005), in accordance with what is found on average from the present study. Granitoids from the ERS region could then be associated with Byrd Coast granite and Ford granodiorite suites, as well as with the Granite Harbour Intrusive Complex from the southern Transantarctic Mountains, that are partially shed into the Mercer and Whillans ice streams (Fig. 7). The major occurrence of granitoids in one core from the WRS sector could be ascribed to its relative proximity with the Southern Victoria Land coast (Table 3) which is characterized by widespread Granite Harbour Intrusive Complex outcrops (Cox et al. 2012).

### 5.3. A comparative overview with older sediments in the Ross Sea

The gravel dataset across a W-E Ross Sea transect was analyzed to identify petrographic provinces that reflect different source regions, providing constraints in the late Quaternary (LGM) ice flows pathways. A look to deep drilling cores in the same region allows one to better understand the changes in the clast assemblages through time. In particular, gravel datasets from Oligo-Miocene glacimarine sequences located in the CRS area (from IODP site U1521, Marschalek et al., 2021; Zurli et al., 2022 and DSDP site 270, Olivetti et al., 2023) and from Miocene-Pleistocene diamictites in the WRS (AND-2A and AND-1B, Talarico et al., 2012, Talarico and Sandroni, 2011) were compared with data from this study.

In the critical region of the CRS, marker lithologies that register oscillations of the Transantarctic Mountains and/or West Antarctica detrital contribution during the Early-Middle Miocene are represented by dolerites. Their occurrence drops during West Antarctica provenance dominated intervals, while they are common when sediments were fed by East Antarctica (Marschalek et al., 2021; Zurli et al., 2022; Olivetti et al., 2023). Other minor marker lithologies, such as limestones and marbles, are only present in IODP Site U1521 Miocene intervals with an East Antarctic signature, and informs about central Transantarctic Mountains glaciers' influence on CRS detritus during these stages. Limestone and hybrid carbonate sandstone clasts have been recorded also by Cornamusini and Talarico (2016) in coeval sequences from AND-2A drilling-core, but in this case a primary source area in the Discovery Deep (a 1000m deep elongated depression below the Ross Ice Shelf, in front of Byrd and Mulock glaciers) has been hypothesized. Even if dolerite acts as a provenance marker in the Miocene sediments of the CRS, the comparison with late Quaternary clasts of this study, and other provenance studies in finer granulometric fraction (i.e., Licht et al., 2005), highlights that its occurrence is scarce due to deepening of the valleys in the Transantarctic Mountains front onto the crystalline basement, as pointed out in coastal cores (i.e., CIROS, Sandroni and Talarico, 2004). Indeed, the occurrence of limestone in the CRS could be considered a Transantarctic Mountains provenance marker in the past (Marschaleck et al., 2021; Zurli et al., 2022) and in the late Quaternary, both in the sand (Licht et al., 2005) and in gravel fractions (this study). In contrast to the CRS, in the WRS volcanic rocks likely eroded from the volcanic centers of the Erebus Volcanic Province are the dominant detrital lithology during the Early-Middle Miocene intervals (Sandroni and Talarico 2011; Talarico and Sandroni 2011).

Compared to the LGM WRS record, these intervals are richer in volcanic detritus and also in Ferrar Group rocks, even if the proximity of the core to volcanic centers strongly influence it.

As a general trend, the pebble abundance data in the WRS record progressive glacial incision into the Transantarctic Mountains. In the McMurdo sound area, drill-cores records up-core decrease of Ferrar Group rocks in the gravel fraction (Talarico et al., 2000; Sandroni and Talarico, 2004; Talarico et al. 2012) relative to the abundance of metamorphic rock clasts. These low-grade metasediments (meta-sandstones, meta-siltstones, meta-limestones and phyllites), and in some cases medium to high grade rocks such as para- and ortho-gneisses, indicate a source region located between Skelton-Mulock glaciers and Carlyon-Darwin glaciers. Ferrar Rocks are usually found together with Beacon Supergroup sandstones in the gravel fraction from Oligocene-Miocene sediments in the WRS, but both rock types register a reduction since the Pliocene in AND-2A (Cornamusini and Talarico 2016). This means that glacial erosion in the source areas proceeded first on the cover units represented by Beacon and Ferrar supergroups, and then progressively on the basement units represented by GHIC lithologies and the associated metamorphic rocks. Thus, during the Early-Middle Miocene, more dolerites and sandstones were available for providing detritus in a distal area (CRS), while during the Quaternary their contribution is smaller and crystalline basement lithologies constitute the majority of pebbles. This is also in accordance with the geochronological findings of Licht and Palmer (2013), showing that Ross Sea LGM tills reflect input from downstream and upstream glacier areas, highlighting the complexity of erosion patterns along a single outlet glaciers profile. The progressive deepening caused by erosion along the axis of the glaciers must therefore have led to a change in the gravel assemblage from the Miocene to the Quaternary as underlying lithologies were encountered.

In sum, the main fingerprint in the WRS clast assemblage is the abundance of volcanic clasts related with the McMurdo Volcanic Group; their occurrence is ubiquitous both in the Miocene-Pliocene strata of the ANDRILL cores, and in the late Quaternary gravel of this study and also in the sand fraction (Licht et al., 2005). On the contrary, the composition of the pre-Cenozoic rocks constituting the Transantarctic Mountains varies through time on the basis of both deepening of the valleys and the source shifts from more proximal outlet glaciers to more southern ones.

## 6. Conclusions

A petrographic study has been carried out for the first time in a systematic way on gravel clasts from LGM subglacial-ice proximal glacigenic sediments in the eastern, central, and western Ross Sea representing direct glacial transport. This study identifies three petrofacies, variably composed of metasedimentary, intrusives, sedimentary, and volcanic rocks. Mineral paragenesis of the most abundant meta-sedimentary rocks suggest a sub-greenschist/greenschist metamorphic grade, which indicates a terrain subjected to low grade metamorphism as the main source area.

The presence of rare but significant lithologies such as carbonate rocks (limestones and marbles) acts as a marker to identify likely source areas, identified in particular, but not exclusively, in the region of central Transantarctic Mountains.

The abundant occurrence of volcanic lithotypes mainly derived from dismantling of McMurdo Volcanic Group rocks is limited to the Western Ross Sea sector, with a glaciological divide represented by the Ross Bank area, east of which the detrital gravel fraction lacks a prominent volcanic composition.

This study demonstrates, in accordance with previous multianalytical provenance studies on sand fraction, that during late Quaternary, the CRS is the convergence area of ice discharged from the central and southern Transantarctic Mountains region and from West Antarctic Ice Streams, with clast assemblages revealing sources located from both sides of the Ross Sea Embayment.

The comparison of the late Quaternary gravel dataset with the same fraction from older glacigenic sediments in the central and western Ross Sea emphasizes in general the role of glacial erosion in determining lithotypes associations and highlights changes in marker lithologies (i.e. dolerites) between past and recent glacial scenarios.



## Acknowledgments

This work was mainly supported by the Italian “Programma Nazionale di Ricerche in Antartide (PNRA)” [grant number PNRA 2013/AZ2.08]. We wish to thank the staff of the Marine Geology Antarctic Research Facility of Tallahassee, Florida, where the studied cores were stored. Our acknowledgement also goes to the staff of the Siena section of the “Museo Nazionale dell’Antartide”. We also wish to thank the Editor Catherine Chagué and the two anonymous reviewers which helped to improve the manuscript with their constructive comments.

## References

Adams, C.J., 1986. Geochronological studies of the Swanson Formation of Marie Byrd Land, West Antarctica, and correlation with northern Victoria Land, East Antarctica, and South Island, New Zealand. New Zeal. J. Geol. Geophys. 29, 345–358. https://doi.org/10.1080/00288306.1986.10422157

Adams, C.J., Mortimer, N., Campbell, H.J., Griffin, W.L., 2013. The mid-Cretaceous transition from basement to cover within sedimentary rocks in eastern New Zealand: evidence from detrital zircon age patterns. Geol. Mag. 150, 455–478. https://doi.org/10.1017/S0016756812000611

Albrecht, T., Winkelmann, R., Levermann, A., 2020. Glacial-cycle simulations of the Antarctic Ice Sheet with the Parallel Ice Sheet Model (PISM)-Part 2: Parameter ensemble analysis. Cryosphere 14, 633–656. https://doi.org/10.5194/TC-14-633-2020

Allibone, A., Wysoczanski, R., 2002. Initiation of magmatism during the Cambrian–Ordovician Ross orogeny in southern Victoria Land, Antarctica. Geol. Soc. Am. Bull. 114, 1007–1018. https://doi.org/10.1130/0016-7606(2002)114<1007:IOMDTC>2.0.CO;2

Anderson, J.B., 1999. Antarctic Marine Geology. Antarct. Mar. Geol. https://doi.org/10.1017/CBO9780511759376

Anderson, J.B., Brake, C.F., Myers, N.C., 1984. Sedimentation on the Ross Sea continental shelf, Antarctica. Mar. Geol. 57, 295–333. https://doi.org/10.1016/0025-3227(84)90203-2

Anderson, J.B., Conway, H., Bart, P.J., Witus, A.E., Greenwood, S.L., McKay, R.M., Hall, B.L., Ackert, R.P., Licht, K., Jakobsson, M., Stone, J.O., 2014. Ross Sea paleo-ice sheet drainage and deglacial history during and since the LGM. Quat. Sci. Rev. 100, 31–54. https://doi.org/10.1016/j.quascirev.2013.08.020

Anderson, J.B., Shipp, S.S., Bartek, L.R., Reid, D.E., 1992. Evidence for a grounded ice sheet on the Ross Sea continental shelf during the Late Pleistocene and preliminary paleodrainage reconstruction, in: Elliot, D.H. (Ed.), Contributions to Antarctic Research III. American Geophysical Union (AGU), pp. 39–62. https://doi.org/10.1029/AR057p0039

Anderson, J.B., Shipp, S.S., Lowe, A.L., Wellner, J.S., Mosola, A.B., 2002. The Antarctic Ice Sheet during the Last Glacial Maximum and its subsequent retreat history: a review. Quat. Sci. Rev. 21, 49–70. https://doi.org/10.1016/S0277-3791(01)00083-X

Andrews, J.T., LeMasurier, W., 2021. Resolving the argument about volcanic bedrock under the West Antarctic Ice Sheet and implications for ice sheet stability and sea level change. Earth Planet. Sci. Lett. 568, 117035. https://doi.org/10.1016/J.EPSL.2021.117035

Balestrieri, M.L., Olivetti, V., Chew, D., Zurli, L., Zattin, M., Drakou, F., Cornamusini, G., Perotti, M., 2024. Recurrent E - W oscillations of the ice flow confluence of the East and West Antarctic ice sheets in the central Ross Sea, Antarctica, from the Middle Miocene to the present day. Palaeogeogr. Palaeoclimatol. Palaeoecol. 633, 111885. https://doi.org/10.1016/J.PALAEO.2023.111885

Ballance, P.F., Waiters, W.A., 2002. Hydrothermal alteration, contact metamorphism, and authigenesis in Ferrar Supergroup and Beacon Supergroup rocks, Carapace Nunatak, Allan Hills, and Coombs Hills, Victoria Land, Antarctica. New Zeal. J. Geol. Geophys. 45, 71–84. https://doi.org/10.1080/00288306.2002.9514960

Barrett, P.J., 1991. The Devonian to Jurassic Beacon Supergroup of the Transantarctic Mountains and correlatives in other parts of Antarctica, in: Tingey, R.J. (Ed.), The Geology of Antarctica. Clarendon Press, Oxford, pp. 120–152.

Barrett, P.J., 1966. Petrology of some Beacon rocks between the Axel Heiberg and Shackleton glaciers, Queen Maud Range, Antarctica. J. Sediment. Petrol. 36, 794–805

Bernet, M., Gaupp, R., 2005. Diagenetic history of Triassic sandstone from the Beacon Supergroup in central Victoria Land, Antarctica. New Zeal. J. Geol. Geophys. 48, 447–458. https://doi.org/10.1080/00288306.2005.9515125

Bradshaw, J.D., Andrews, P.B., Field, B.D., 1983. Swanson Formation and related rocks of Marie Byrd Land and a comparison with the Robertson Bay Group of northern Victoria Land, in: Oliver, R.L., James, P.R., Jago, J. (Eds.), Antarctic Earth Science. Australian Academy of Science, Canberra, pp. 274–279.

Brand, J.F., 1979. Low Grade Metamorphic Rocks of the Ruppert and Hobbs Coasts of Marie Byrd Land, Antarctica. Tex. Tech University

Carosi, R., Giacomini, F., Talarico, F.M., Stump, E., 2007. Geology of the Byrd Glacier Discontinuity (Ross Orogen): New survey data from the Britannia Range, Antarctica, in: Cooper, A.K., Raymond, C.R. (Eds.), A Keystone in a Changing World - Online Proceedings of the 10th ISAES. U.S. Geological Survey and The National Academies. https://doi.org/10.3133/ofr20071047SRP030

Cook, Y.A., Craw, D., 2002. Neoproterozoic structural slices in the Ross Orogen, Skelton Glacier area, South Victoria Land, Antarctica. New Zeal. J. Geol. Geophys. 45, 133–143. https://doi.org/10.1080/00288306.2002.9514965

Cook, Y.A., Craw, D., 2001. Amalgamation of disparate crustal fragments in the Walcott Bay-Foster Glacier area, South Victoria Land, Antarctica. New Zeal. J. Geol. Geophys. 44, 403–416. https://doi.org/10.1080/00288306.2001.9514947

Cornamusini, G., Talarico, F.M., 2016. Miocene Antarctic ice dynamics in the Ross Embayment (Western Ross Sea, Antarctica): Insights from provenance analyses of sedimentary clasts in the AND-2A drill core. Glob. Planet. Change 146, 38–52. https://doi.org/10.1016/j.gloplacha.2016.09.001

Cornamusini, G., Zurli, L., Liberato, G.P., Corti, V., Gulbranson, E.L., Perotti, M., Sandroni, S., 2023. A lithostratigraphic reappraisal of a Permian-Triassic fluvial succession at Allan Hills (Antarctica) and implications for the terrestrial end-Permian extinction event. Palaeogeogr. Palaeoclimatol. Palaeoecol. 627, 111741. https://doi.org/10.1016/J.PALAEO.2023.111741

Cottle, John M, Cooper, A.F., 2006. The Fontaine Pluton: An early Ross Orogeny calc-alkaline gabbro from southern Victoria Land, Antarctica. New Zeal. J. Geol. Geophys. 49, 177–189. https://doi.org/10.1080/00288306.2006.9515158

Cottle, John M., Cooper, A.F., 2006. Geology, geochemistry, and geochronology of an A-type granite in the Mulock Glacier area, southern Victoria Land, Antarctica. New Zeal. J. Geol. Geophys. 49, 191–202. https://doi.org/10.1080/00288306.2006.9515159

Cox, S.C., Smith Lyttle, B., Elkind, S., Smith Siddoway, C., Morin, P., Capponi, G., Abu-Alam, T., Ballinger, M., Bamber, L., Kitchener, B., Lelli, L., Mawson, J., Millikin, A., Dal Seno, N., Whitburn, L., White, T., Burton-Johnson, A., Crispini, L., Elliot, D., Elvevold, S., Goodge, J., Halpin, J., Jacobs, J., Martin, A.P., Mikhalsky, E., Morgan, F., Scadden, P., Smellie, J., Wilson, G., 2023. A continent-wide detailed geological map dataset of Antarctica. Sci. Data 2023 101 10, 1–14. https://doi.org/10.1038/s41597-023-02152-9

Cox, S.C., Turnbull, I.M., Isaac, M.J., Townsend, D.B., Lyttle, B.S., 2012. Geology of southern Victoria Land Antarctica, Institute. ed, Institute of Geological and Nuclear Sciences 1:250,000 Geological Map. Lower Hutt, New Zealand.

Danielson, M.A., Bart, P.J., 2024. The staggered retreat of grounded ice in the Ross Sea, Antarctica, since the Last Glacial Maximum (LGM). Cryosphere 18, 1125–1138. https://doi.org/10.5194/TC-18-1125-2024

Denton, G.H., Hughes, T.J., 2002. Reconstructing the Antarctic Ice Sheet at the Last Glacial Maximum. Quat. Sci. Rev. 21, 193–202. https://doi.org/10.1016/S0277-3791(01)00090-7

Denton, G.H., Hughes, T.J., 2000. Reconstruction of the Ross Ice Drainage System, Antarctica, at the Last Glacial Maximum. Geogr. Ann. Ser. A, Phys. Geogr. 82, 143–166. https://doi.org/10.1111/J.0435-3676.2000.00120.X

Deschamps, P., Durand, N., Bard, E., Hamelin, B., Camoin, G., Thomas, A.L., Henderson, G.M., Okuno, J., Yokoyama, Y., 2012. Ice-sheet collapse and sea-level rise at the Bølling warming 14,600 years ago. Nature 483, 559–564. https://doi.org/10.1038/nature10902

Droop, G.T.R., 1987. A general equation for estimating Fe 3+ concentrations in ferromagnesian silicates and oxides from microprobe analyses, using stoichiometric criteria. Mineral. Mag. 51, 431–435. https://doi.org/10.1180/minmag.1987.051.361.10

Elliot, D.H., Fleming, T.H., 2021. Ferrar Large Igneous Province: petrology, in: Smellie, J.L., Panter, K.S., Geyer, A. (Eds.), Volcanism in Antarctica: 200 Million Years of Subduction, Rifting and Continental Break-Up. pp. 93–119. https://doi.org/10.1144/M55-2018-39

Elliot, D.H., White, J.D.L., Fleming, T.H., 2021. Ferrar Large Igneous Province: volcanology, in: Smellie, J.L., Panter, K.S., Geyer, A. (Eds.), Volcanism in Antarctica: 200 Million Years of Subduction, Rifting and Continental Break-Up. Geological Society of London, London, pp. 75–91. https://doi.org/10.1144/M55-2018-4

Encarnación, J., Grunow, A., 1996. Changing magmatic and tectonic styles along the paleo-Pacific margin of Gondwana and the onset of early Paleozoic magmatism in Antarctica. Tectonics 15, 1325–1341. https://doi.org/10.1029/96TC01484

Estrada, S., Läufer, A., Eckelmann, K., Hofmann, M., Gärtner, A., Linnemann, U., 2016. Continuous Neoproterozoic to Ordovician sedimentation at the East Gondwana margin — Implications from detrital zircons of the Ross Orogen in northern Victoria Land, Antarctica. Gondwana Res. 37, 426–448. https://doi.org/10.1016/j.gr.2015.10.006

Farmer, G., Licht, K.J., Swope, R., Andrews, J., 2006. Isotopic constraints on the provenance of fine-grained sediment in LGM tills from the Ross Embayment, Antarctica. Earth Planet. Sci. Lett. 249, 90–107. https://doi.org/10.1016/j.epsl.2006.06.044

Farmer, G.L., Licht, K.J., 2016. Generation and fate of glacial sediments in the central Transantarctic Mountains based on radiogenic isotopes and implications for reconstructing past ice dynamics. Quat. Sci. Rev. 150, 98–109. https://doi.org/10.1016/J.QUASCIREV.2016.08.002

Findlay, R.H., Craw, D., Skinner, D.N.B., 1984. Lithostratigraphy and structure of the Koettlitz Group, McMurdo Sound, Antarctica. New Zeal. J. Geol. Geophys. 27, 513–536. https://doi.org/10.1080/00288306.1984.10422270

Geyer, A., Di Roberto, A., Smellie, J.L., Van Wyk de Vries, M., Panter, K.S., Martin, A.P., Cooper, J.R., Young, D., Pompilio, M., Kyle, P.R., Blankenship, D., 2023. Volcanism in Antarctica: An assessment of the present state of research and future directions. J. Volcanol. Geotherm. Res. 444, 107941. https://doi.org/10.1016/J.JVOLGEORES.2023.107941

Golledge, N.R., Fogwill, C.J., Mackintosh, A.N., Buckley, K.M., 2012. Dynamics of the last glacial maximum Antarctic ice-sheet and its response to ocean forcing. Proc. Natl. Acad. Sci. 109, 16052–16056. https://doi.org/10.1073/pnas.1205385109

Golledge, N.R., Levy, R.H., McKay, R.M., Fogwill, C.J., White, D.A., Graham, A.G.C., Smith, J.A., Hillenbrand, C.-D., Licht, K.J., Denton, G.H., Ackert, R.P., Maas, S.M., Hall, B.L.,

2013. Glaciology and geological signature of the Last Glacial Maximum Antarctic ice sheet. Quat. Sci. Rev. 78, 225–247. https://doi.org/10.1016/j.quascirev.2013.08.011

Goodge, J.W., 2020. Geological and tectonic evolution of the Transantarctic Mountains, from ancient craton to recent enigma. Gondwana Res. 80, 50–122. https://doi.org/10.1016/j.gr.2019.11.001

Goodge, J.W., Fanning, C.M., 2016. Mesoarchean and Paleoproterozoic history of the Nimrod Complex, central Transantarctic Mountains, Antarctica: Stratigraphic revisions and relation to the Mawson Continent in East Gondwana. Precambrian Res. 285, 242–271. https://doi.org/10.1016/j.precamres.2016.09.001

Goodge, J.W., Hansen, V.L., Peacock, S.M., Smith, B.K., Walker, N.W., 1993. Kinematic evolution of the Miller Range Shear Zone, Central Transantarctic Mountains, Antarctica, and implications for Neoproterozoic to Early Paleozoic tectonics of the East Antarctic Margin of Gondwana. Tectonics 12, 1460–1478. https://doi.org/10.1029/93TC02192

Goodge, J.W., Mark Fanning, C., 1999. 2.5 b.y. of punctuated Earth history as recorded in a single rock. Geology 27, 1007–1010. https://doi.org/10.1130/0091-7613(1999)027<1007:BYOPEH>2.3.CO;2

Goodge, J.W., Myrow, P., Williams, I.S., Bowring, S.A., 2002. Age and Provenance of the Beardmore Group, Antarctica: Constraints on Rodinia Supercontinent Breakup. J. Geol. 110, 393–406.

Gunn, B.M., Warren, G., 1962. Geology of Victoria Land between the Mawson and Mulock Glaciers, Antarctica, New Zealand Geological Survey Bulletin.

Halberstadt, A.R.W., Simkins, L.M., Greenwood, S.L., Anderson, J.B., 2016. Past ice-sheet behaviour: retreat scenarios and changing controls in the Ross Sea, Antarctica. Cryosph. 10, 1003–1020. https://doi.org/10.5194/tc-10-1003-2016

Hauptvogel, D.W., Passchier, S., 2012. Early–Middle Miocene (17–14Ma) Antarctic ice dynamics reconstructed from the heavy mineral provenance in the AND-2A drill core, Ross Sea, Antarctica. Glob. Planet. Change 82–83, 38–50. https://doi.org/10.1016/j.gloplacha.2011.11.003

Hughes, T., 1977. West Antarctic ice streams. Rev. Geophys. 15, 1–46. https://doi.org/10.1029/RG015I001P00001

Huybrechts, P., 2002. Sea-level changes at the LGM from ice-dynamic reconstructions of the Greenland and Antarctic ice sheets during the glacial cycles. Quat. Sci. Rev. 21, 203–231. https://doi.org/10.1016/S0277-3791(01)00082-8

Jordan, T.A., Riley, T.R., Siddoway, C.S., 2020. The geological history and evolution of West Antarctica. Nat. Rev. Earth Environ. 1, 117–133. https://doi.org/10.1038/s43017-019-0013-6

Laird, M.., 1991. The Late Proterozoic-Middle Palaeozoic rocks of Antarctica, in: Tingey, R.J. (Ed.), The Geology of Antarctica. pp. 74–119.

Laird, M.G., Mansergh, G.D., Chappell, J.M.A., 1971. Geology of the Central Nimrod Glacier area, Antarctica. New Zeal. J. Geol. Geophys. 14, 427–468. https://doi.org/10.1080/00288306.1971.10421939

Leake, B.E., Woolley, A.R., Arps, C.E.S., Birch, W.D., Gilbert, M.C., Grice, J.D., Hawthorne, F.C., Kato, A., Kisch, H.J., Krivovichev, V.G., Linthout, K., Laird, J., Mandarino, J.A., Maresch, W. V, Nickel, E.H., Schumacher, J.C., Smith, D.C., Stephenson, N.C.N., Ungaretti, L., Whittaker, E.J.W., Youzhi, G., 1997. Nomenclature of amphiboles: report of the subcommittee on amphiboles of the international mineralogical association, commissiion on new minerals and mineral names. Can. Mineral. 35, 219–246.

LeMasurier, W.E., Choi, S.H., Kawachi, Y., Mukasa, S.B., Rogers, N.W., 2011. Evolution of pantellerite-trachyte-phonolite volcanoes by fractional crystallization of basanite magma in a continental rift setting, Marie Byrd Land, Antarctica. Contrib. to Mineral. Petrol. 162, 1175–1199. https://doi.org/10.1007/s00410-011-0646-z

LeMasurier, W.E., Landis, C.A., 1996. Mantle-plume activity recorded by low-relief erosion surfaces in West Antarctica and New Zealand. Geol. Soc. Am. Bull. 108, 1450–1466. https://doi.org/10.1130/0016-7606(1996)108<1450:MPARBL>2.3.CO;2

Levy, R.H., Harwood, D.M., 2000. Sedimentary lithofacies of the McMurdo sound erratics, in: Stilwel, J.D., Feldman, R.M. (Eds.), Paleobiology and Paleoenvironments of Eocene Rocks: McMurdo Sound, East Antarctica. American Geophysical Union (AGU), pp. 39–61. https://doi.org/10.1029/AR076p0039

Li, X., Zattin, M., Olivetti, V., 2020. Apatite Fission Track Signatures of the Ross Sea Ice Flows During the Last Glacial Maximum. Geochemistry, Geophys. Geosystems 21. https://doi.org/10.1029/2019GC008749

Licht, K.J., Andrews, J.T., 2002. The 14 C Record of Late Pleistocene Ice Advance and Retreat in the Central Ross Sea, Antarctica. Arctic, Antarct. Alp. Res. 34, 324–333. https://doi.org/10.1080/15230430.2002.12003501

Licht, K.J., Dunbar, G., Andrews, J.T., Jennings, A.E., 1999. Distinguishing subglacial till and glacial marine diamictons in the western Ross Sea, Antarctica: Implications for a last

glacial maximum grounding line. Geol. Soc. Am. Bull. 111, 91–103. https://doi.org/https://doi.org/10.1130/0016-7606(1999)111<0091:DSTAGM>2.3.CO;2

Licht, K.J., Hemming, S.R., 2017. Analysis of Antarctic glacigenic sediment provenance through geochemical and petrologic applications. Quat. Sci. Rev. 164, 1–24. https://doi.org/10.1016/j.quascirev.2017.03.009

Licht, K.J., Hennessy, A.J., Welke, B.M., 2014. The U-Pb detrital zircon signature of West Antarctic ice stream tills in the Ross embayment, with implications for Last Glacial Maximum ice flow reconstructions. Antarct. Sci. 26, 687–697. https://doi.org/10.1017/S0954102014000315

Licht, K.J., Lederer, J.R., Jeffrey Swope, R., 2005. Provenance of LGM glacial till (sand fraction) across the Ross embayment, Antarctica. Quat. Sci. Rev. 24, 1499–1520. https://doi.org/10.1016/j.quascirev.2004.10.017

Licht, K.J., Palmer, E.F., 2013. Erosion and transport by Byrd Glacier, Antarctica during the Last Glacial Maximum. Quat. Sci. Rev. 62, 32–48. https://doi.org/10.1016/J.QUASCIREV.2012.11.017

Luyendyk, B.P., Wilson, D.S., Siddoway, C.S., 2003. Eastern margin of the Ross Sea Rift in western Marie Byrd Land, Antarctica: Crustal structure and tectonic development. Geochemistry, Geophys. Geosystems 4. https://doi.org/10.1029/2002GC000462

Marschalek, J.W., Blard, P. -H., Sarigulyan, E., Ehrmann, W., Hemming, S.R., Thomson, S.N., Hillenbrand, C. -D., Licht, K., Tison, J. -L., Ardoin, L., Fripiat, F., Allen, C.S., Marrocchi, Y., Siegert, M.J., van de Flierdt, T., 2024. Byrd Ice Core Debris Constrains the Sediment Provenance Signature of Central West Antarctica. Geophys. Res. Lett. 51. https://doi.org/10.1029/2023GL106958

Marschalek, J.W., Zurli, L., Talarico, F., van de Flierdt, T., Vermeesch, P., Carter, A., Beny, F., Bout-Roumazeilles, V., Sangiorgi, F., Hemming, S.R., Pérez, L.F., Colleoni, F., Prebble, J.G., van Peer, T.E., Perotti, M., Shevenell, A.E., Browne, I., Kulhanek, D.K., Levy, R., Harwood, D., Sullivan, N.B., Meyers, S.R., Griffith, E.M., Hillenbrand, C.-D., Gasson, E., Siegert, M.J., Keisling, B., Licht, K.J., Kuhn, G., Dodd, J.P., Boshuis, C., De Santis, L., McKay, R.M., Ash, J., Beny, F., Browne, I.M., Cortese, G., De Santis, L., Dodd, J.P., Esper, O.M., Gales, J.A., Harwood, D.M., Ishino, S., Keisling, B.A., Kim, Sookwan, Kim, Sunghan, Kulhanek, D.K., Laberg, J.S., Leckie, R.M., McKay, R.M., Müller, J., Patterson, M.O., Romans, B.W., Romero, O.E., Sangiorgi, F., Seki, O., Shevenell, A.E., Singh, S.M., Cordeiro de Sousa, I.M., Sugisaki, S.T., van de Flierdt, T., van Peer, T.E., Xiao, W., Xiong, Z., 2021. A large West Antarctic Ice Sheet explains early Neogene sea-level amplitude. Nature 600, 450–455. https://doi.org/10.1038/s41586-021-04148-0

Martin, A.P., Cooper, A.F., Dunlap, W.J., 2010. Geochronology of Mount Morning, Antarctica: Two-phase evolution of a long-lived trachyte-basanite-phonolite eruptive center. Bull. Volcanol. 72, 357–371. https://doi.org/10.1007/S00445-009-0319-1/FIGURES/10

McKay, R., Golledge, N.R., Maas, S., Naish, T., Levy, R., Dunbar, G., Kuhn, G., 2016. Antarctic marine ice-sheet retreat in the Ross Sea during the early Holocene. Geology 44, 7–10. https://doi.org/10.1130/G37315.1

McKay, R.M., Dunbar, G.B., Naish, T.R., Barrett, P.J., Carter, L., Harper, M., 2008. Retreat history of the Ross Ice Sheet (Shelf) since the Last Glacial Maximum from deep-basin sediment cores around Ross Island. Palaeogeogr. Palaeoclimatol. Palaeoecol. 260, 245–261. https://doi.org/10.1016/J.PALAEO.2007.08.015

Mercer, J., 1978. West Antarctic ice sheet and $CO_2$ greenhouse effect: a threat of disaster. Nature 271, 321-325. https://doi.org/10.1038/271321a0

Morlighem, M., 2020. MEaSUREs BedMachine Antarctica, Version 2 [Data Set] [WWW Document]. Boulder, Color. USA. NASA Natl. Snow Ice Data Cent. Distrib. Act. Arch. Cent. https://doi.org/https://doi.org/10.5067/E1QL9HFQ7A8M

Morlighem, M., Rignot, E., Binder, T., Blankenship, D., Drews, R., Eagles, G., Eisen, O., Ferraccioli, F., Forsberg, R., Fretwell, P., Goel, V., Greenbaum, J.S., Gudmundsson, H., Guo, J., Helm, V., Hofstede, C., Howat, I., Humbert, A., Jokat, W., Karlsson, N.B., Lee, W.S., Matsuoka, K., Millan, R., Mouginot, J., Paden, J., Pattyn, F., Roberts, J., Rosier, S., Ruppel, A., Seroussi, H., Smith, E.C., Steinhage, D., Sun, B., Broeke, M.R. va. den, Ommen, T.D. va., Wessem, M. van, Young, D.A., 2020. Deep glacial troughs and stabilizing ridges unveiled beneath the margins of the Antarctic ice sheet. Nat. Geosci. 2019 132 13, 132–137. https://doi.org/10.1038/s41561-019-0510-8

Mukasa, S.B., Dalziel, I.W.D., 2000. Marie Byrd Land, West Antarctica: Evolution of Gondwana's Pacific margin constrained by zircon U-Pb geochronology and feldspar common-Pb isotopic compositions. Geol. Soc. Am. Bull. 112, 611–627. https://doi.org/10.1130/0016-7606(2000)112<611:MBLWAE>2.0.CO;2

Myrow, P.M., Pope, M.C., Goodge, J.W., Fischer, W., Palmer, A.R., 2002. Depositional history of pre-Devonian strata and timing of Ross orogenic tectonism in the central Transantarctic Mountains, Antarctica. GSA Bull. 114, 1070–1088. https://doi.org/10.1130/0016-7606(2002)114<1070:DHOPDS>2.0.CO;2

Olivetti, V., Balestrieri, M.L., Chew, D., Zurli, L., Zattin, M., Pace, D., Drakou, F., Cornamusini, G., Perotti, M., 2023. Ice volume variations and provenance trends in the Oligocene-early

Miocene glaciomarine sediments of the Central Ross Sea, Antarctica (DSDP Site 270). Glob. Planet. Change 221, 104042. https://doi.org/10.1016/J.GLOPLACHA.2023.104042

Pankhurst, R.J., Weaver, S.D., Bradshaw, J.D., Storey, B.C., Ireland, T.R., 1998. Geochronology and geochemistry of pre-Jurassic superterranes in Marie Byrd Land, Antarctica. J. Geophys. Res. Solid Earth 103, 2529–2547. https://doi.org/10.1029/97JB02605

Paulsen, T., Encarnación, J., Valencia, V.A., Roti Rotia, J.M., Rasoazanamparany, C., 2011. Detrital U–Pb zircon analysis of an Eocene McMurdo Erratic sandstone, McMurdo Sound, Antarctica. New Zeal. J. Geol. Geophys. 54, 353–360. https://doi.org/10.1080/00288306.2011.582123

Perotti, M., Andreucci, B., Talarico, F., Zattin, M., Langone, A., 2017. Multianalytical provenance analysis of Eastern Ross Sea LGM till sediments (Antarctica): Petrography, geochronology, and thermochronology detrital data. Geochemistry, Geophys. Geosystems 18, 2275–2304. https://doi.org/10.1002/2016GC006728

Perotti, M., Zurli, L., Sandroni, S., Cornamusini, G., Talarico, F., 2018. Provenance of Ross Sea Drift in McMurdo Sound (Antarctica) and implications for middle-Quaternary to LGM glacial transport: New evidence from petrographic data. Sediment. Geol. 371, 41–54. https://doi.org/10.1016/j.sedgeo.2018.04.009

Pollard, D., DeConto, R.M., 2009. Modelling West Antarctic ice sheet growth and collapse through the past five million years. Nature 458, 329–332. https://doi.org/10.1038/nature07809

Read, S.E., Cooper, A.F., Walker, N.W., 2002. Geochemistry and U-Pb geochronology of the Neoproterozoic-Cambrian Koettlitz Glacier alkaline province, Royal Society Range, Transantarctic Mountains, Antarctica, in: 8th International Symposium on Antarctic Earth Sciences. Gamble, J.A., Skinner, D.N.B., Henrys, S.A., pp. 143–151.

Rocchi, S., LeMasurier, W.E., Di Vincenzo, G., 2006. Oligocene to Holocene erosion and glacial history in Marie Byrd Land, West Antarctica, inferred from exhumation of the Dorrel Rock intrusive complex and from volcano morphologies. Geol. Soc. Am. Bull. 118, 991–1005. https://doi.org/10.1130/B25675.1

Rowell, A.J., Gonzales, D.A., McKenna, L.W., Evans, K.R., Stump, E., Ricci, C.A., 1997. Lower Paleozoic rocks in the Queen Maud Mountains: Revised ages and significance, in: Ricci, C.A. (Ed.), The Antarctic Region: Geological Evolution and Processes. Terra Antarctica Publication, Siena, pp. 201–207.

Rowell, A.J., Rees, M.N., 1989. Early Palaeozoic history of the upper Beardmore Glacier area: implications for a major Antarctic structural boundary within the Transantarctic Mountains. Antarct. Sci. 1, 249–260. https://doi.org/10.1017/S0954102089000374

Rowell, A.J., Rees, M.N., Evans, K.R., 1992. Evidence of major Middle Cambrian deformation in the Ross orogen, Antarctica. Geology 20, 31–34. https://doi.org/10.1130/0091-7613(1992)020<0031:EOMMCD>2.3.CO;2

Saito, S., Brown, M., Korhonen, F.J., McFadden, R.R., Siddoway, C.S., 2013. Petrogenesis of Cretaceous mafic intrusive rocks, Fosdick Mountains, West Antarctica: Melting of the sub-continental arc mantle along the Gondwana margin. Gondwana Res. 23, 1567–1580. https://doi.org/10.1016/j.gr.2012.08.002

Sandroni, S., Talarico, F., 2004. Petrography and provenance of basement clasts in CIROS-1 core, McMurdo Sound, Antarctica. Terra Antart. 11, 93–114.

Sandroni, S., Talarico, F.M., 2011. The record of Miocene climatic events in AND-2A drill core (Antarctica): Insights from provenance analyses of basement clasts. Glob. Planet. Change 75, 31–46. https://doi.org/10.1016/j.gloplacha.2010.10.002

Shipp, S.S., Anderson, J.B., Domack, E.W., 1999. Late Pleistocene–Holocene retreat of the West Antarctic Ice-Sheet system in the Ross Sea: Part 1—Geophysical results. Geol. Soc. Am. Bull. 111, 1486–1516. https://doi.org/10.1130/0016-7606(1999)111<1486:LPHROT>2.3.CO;2

Siddoway, C.S., 2008. Tectonics of the West Antarctic rift system: new light on the history and dynamics of distributed intracontinental extension, in: Cooper, A.K., Barrett, P.J., Stagg, H., Storey, B., Stump, E., Wise, W. (Eds.), Antarctica: A Keystone in a Changing World. Proceedings of the 10th International Symposium on Antarctic Earth Sciences. Washington, DC. https://doi.org/10.3133/ofr20071047KP09

Siddoway, C.S., Richard, S.M., Fanning, C.M., Luyendyk, B.P., 2004. Origin and emplacement of a middle Cretaceous gneiss dome, Fosdick Mountains, West Antarctica, in: Gneiss Domes in Orogeny. Geological Society of America, pp. 267–294. https://doi.org/10.1130/0-8137-2380-9.267

Simpson, A.L., Cooper, A.F., 2002. Geochemistry of the Darwin Glacier region granitoids, southern Victoria Land. Antarct. Sci. 14, 425–426. https://doi.org/10.1017/S0954102002000226

Simpson, G., Aslund, T., 1996. Diorite and gabbro of the Dromedary mafic complex, South Victoria Land, Antarctica. New Zeal. J. Geol. Geophys. 39, 403–414. https://doi.org/10.1080/00288306.1996.9514722

Skinner, D.N.B., 1983. The granites of two orogenies of southern Victoria Land, in: Oliver, P.B., James, P.R., Jago, J.B. (Eds.), Antarctic Earth Science. Australian Academy of Science, Camberra, pp. 160–163.

Skinner, D.N.B., 1982. Stratigraphy and structure of low-grade metasedimentary rocks of the Skelton Group, Southern Victoria Land - does Teall Greywacke really exist ( Antarctica)?, in: Antarctic Geoscience. 3rd Symposium on Antarctic Geology and Geophysics, Madison, August 1977. University of Wisconsin Press, pp. 555–563.

Skinner, D.N.B., 1965. Petrographic criteria of the rock units between the Byrd and Starshot Glaciers, South Victoria land, Antarctica. New Zeal. J. Geol. Geophys. 8, 292–303. https://doi.org/10.1080/00288306.1965.10428112

Skinner, D.N.B., 1964. A summary of the geology of the region between Byrd and Starshot glaciers, south Victoria Land, in: Adie, R.J. (Ed.), Antarctic Geology. Amsterdam.

Smellie, J.L., Martin, A.P., 2021. Erebus Volcanic Province: volcanology, in: Smellie, J.L., Panter, K.S., Geyer, A. (Eds.), Geological Society, London, Memoirs. Geological Society of London, pp. 415–446. https://doi.org/10.1144/M55-2018-62

Smellie, J.L., Panter, K.S., Geyer, A., 2021. Introduction to volcanism in Antarctica: 200 million years of subduction, rifting and continental break-up. Geol. Soc. London, Mem. 55, 1–6. https://doi.org/10.1144/M55-2020-14

Smellie, J.L., Rocchi, S., 2021. Northern Victoria Land: volcanology, in: Smellie, J.L., Panter, K.S., Geyer, A. (Eds.), Geological Society, London, Memoirs. pp. 347–381. https://doi.org/10.1144/M55-2018-60

Storey, B.C., Leat, P.T., Weaver, S.D., Pankhurst, R.J., Bradshaw, J.D., Kelley, S., 1999. Mantle plumes and Antarctica-New Zealand rifting: Evidence from mid-Cretaceous mafic dykes. J. Geol. Soc. London. 156, 659–671. https://doi.org/10.1144/GSJGS.156.4.0659

Stump, E., 1995. The Ross orogen of the Transantarctic Mountains. Cambridge University Press, Cambridge.

Stump, E., 1986. Stratigraphy of the Ross Supergroup, central Transantarctic Mountains, in: Turner, M.D., Splettstoesser, J.E. (Eds.), Geology of the Central Transantarctic Mountains: Antarctic Research Series, American Geophysical Union. pp. 225–274. https://doi.org/10.1029/AR036p0225

Stump, E., 1982. the Ross Supergroup in the Queen Maud Mountains, in: Craddock, C. (Ed.), Antarctic Geoscience. University of Wisconsin Press, Madison, pp. 565–569.

Stump, E., 1981. Structural relationships in the Duncan Mountains, central Transantarctic Mountains, Antarctica. New Zeal. J. Geol. Geophys. 24, 87–93. https://doi.org/10.1080/00288306.1981.10422699

Stump, E., Gootee, B.F., Talarico, F., Van Schmus, W.R., Brand, P.K., Foland, K.A., Fanning, C.M., 2004. Correlation of Byrd and Selborne Groups, with implications for the Byrd Glacier discontinuity, central Transantarctic Mountains, Antarctica. New Zeal. J. Geol. Geophys. 47, 157–171. https://doi.org/10.1080/00288306.2004.9515045

Talarico, F., Ghezzo, C., Kleinschmidt, G., 2022. The Antarctic Continent in Gondwana: a perspective from the Ross Embayment and Potential Research Targets for Future Investigations, in: Florindo, F., Siegert, M., Naish, T.R. (Eds.), Antarctic Climate Evolution. Elsevier, pp. 219–296. https://doi.org/10.1016/B978-0-12-819109-5.00004-9

Talarico, F., Sandroni, S., Fielding, C., Atkins, C., 2000. Variability, petrography and provenance of basement clasts in core from CRP-2/2A, Victoria land Basin, Antarctica. Terra Antarct. 7, 529–544.

Talarico, F.M., McKay, R.M., Powell, R.D., Sandroni, S., Naish, T., 2012. Late Cenozoic oscillations of Antarctic ice sheets revealed by provenance of basement clasts and grain detrital modes in ANDRILL core AND-1B. Glob. Planet. Change 96–97, 23–40. https://doi.org/10.1016/j.gloplacha.2009.12.002

Talarico, F.M., Pace, D., Levy, R.H., 2013. Provenance of basement erratics in Quaternary coastal moraines, southern McMurdo Sound, and implications for the source of Eocene sedimentary rocks. Antarct. Sci. 25, 681–695. https://doi.org/10.1017/S0954102013000072

Talarico, F.M., Sandroni, S., 2011. Early Miocene basement clasts in ANDRILL AND-2A core and their implications for paleoenvironmental changes in the McMurdo Sound region (western Ross Sea, Antarctica). Glob. Planet. Change 78, 23–35. https://doi.org/10.1016/j.gloplacha.2011.05.002

Talarico, F.M., Sandroni, S., 2009. Provenance signatures of the Antarctic Ice Sheets in the Ross Embayment during the Late Miocene to Early Pliocene: The ANDRILL AND-1B core record. Glob. Planet. Change 69, 103–123. https://doi.org/10.1016/j.gloplacha.2009.04.007

Talarico, F.M., Stump, E., Gootee, B.F., Foland, K.A., Palmeri, R., Van Schmus, W.R., Brand, P.K., Ricci, C.A., 2007. First evidence of a “Barrovian”-type metamorphic regime in the Ross orogen of the Byrd Glacier area, central Transantarctic Mountains. Antarct. Sci. 19, 451–470. https://doi.org/10.1017/S0954102007000594

The Polar Rock Repository (PRR), Byrd Polar and Climate Research Center (BPCRC), O.S.U., 2015. Geological samples available for research from the PRR. NOAA National Centers for Environmental Information [date of access 2024/05/10]. https://doi.org/10.7289/V5RF5S18

Van Wyk De Vries, M., Bingham, R.G., Hein, A.S., 2018. A new volcanic province: An inventory of subglacial volcanoes in West Antarctica. Geol. Soc. Spec. Publ. 461, 231–248. https://doi.org/10.1144/SP461.7/ASSET/BA1D4A97-7C0A-4A78-AF8D-08CFE011349C/ASSETS/GRAPHIC/SP461-1959F05.JPEG

Vogel, S.W., Tulaczyk, S., Carter, S., Renne, P., Turrin, B., Grunow, A., 2006. Geologic constraints on the existence and distribution of West Antarctic subglacial volcanism. Geophys. Res. Lett. 33. https://doi.org/10.1029/2006GL027344

Weaver, S.D., Adams, C.J., Pankhurst, R.J., Gibson, I.L., 1992. Granites of Edward VII Peninsula, Marie Byrd Land: anorogenic magmatism related to Antarctic-New Zealand rifting. Earth Environ. Sci. Trans. R. Soc. Edinburgh 83, 281–290. https://doi.org/10.1017/S0263593300007963

Weaver, S.D., Bradshaw, J.D., Adams, C.J., 1991. Granitoids of the Ford Ranges, Marie Byrd Land, Antarctica, in: Geological Evolution of Antarctica. M. R. A. Thompson et al., Cambridge, pp. 345–351.

Weaver, S.D., Storey, B.C., Pankhurst, R.J., Mukasa, S.B., DiVenere, V.J., Bradshaw, J.D., 1994. Antarctica-New Zealand rifting and Marie Byrd Land lithospheric magmatism linked to ridge subduction and mantle plume activity. Geology 22, 811–814. https://doi.org/10.1130/0091-7613(1994)022<0811:ANZRAM>2.3.CO;2

Whitney, D.L., Evans, B.W., 2010. Abbreviations for names of rock-forming minerals. Am. Mineral. 95, 185–187. https://doi.org/10.2138/am.2010.3371

Wilch, T.I., McIntosh, W.C., Panter, K. S., 2021. Marie Byrd Land and Ellsworth Land: volcanology, in: Smellie, J.L., Panter, Kurt S., Geyer, A. (Eds.), Geological Society, London, Memoirs. Geological Society of London, pp. 515–576. https://doi.org/10.1144/M55-2019-39

Winberry, J.P., Anandakrishnan, S., 2004. Crustal structure of the West Antarctic rift system and Marie Byrd Land hotspot. Geology 32, 977. https://doi.org/10.1130/G20768.1

Wysoczanski, R.J., Forsyth, P.J., Woolfe, K.J., 2003. Zircon dating and provenance of rhyolitic clasts in Beacon Conglomerate, Southern Victoria Land, Antarctica. Terra Antart. 10, 67–80.

Zurli, L., Liberato, G.P., Perotti, M., Woo, J., Lee, M.J., Cornamusini, G., 2024a. A multi-proxy detrital study from Permian-Triassic fluvial sequences of Victoria Land (Antarctica): Implications for the Gondwanan basin evolution. Palaeogeogr. Palaeoclimatol. Palaeoecol. 641, 112113. https://doi.org/10.1016/J.PALAEO.2024.112113

Zurli, L., Perotti, M., Cornamusini, G., 2024b. Composition of Late Paleozoic Ice Age tillites in Victoria Land (Antarctica): implications for sediment provenance and ice centers extent in southern Gondwana. Rend. Online della Soc. Geol. Ital. 63, 1–8. https://doi.org/10.3301/ROL.2024.27

Zurli, L., Perotti, M., Talarico, F.M., 2022. Data report: petrology of gravel-sized clasts from Site U1521 core, IODP Expedition 374, Ross Sea West Antarctic Ice Sheet History, in: McKay, R.M., De Santis, L., Kulhanek, D.K. (Eds.), Proceedings of the International Ocean Discovery Program Volume 374. International Ocean Discovery Program, College Station - TX. https://doi.org/10.14379/IODP.PROC.374.201.2022

**Table Captions**

**Table 1.** List of sample sites. They are shown labeled in other figures and elsewhere in the text. ERS: eastern Ross Sea; Sulz.Bay: Sulzberger Bay; CRS: Central Ross Sea; WRS: Western Ross Sea.

**Table 2.** List of analyzed thin sections, with petrographic features of each clast and piston cores label from which they were sampled. Mineral abbreviations according to Whitney and Evans (2010) except for opm: opaque minerals and wm: white mica. vfg: very fine grained; fg: fine grained; mg: medium grained; cg: coarse grained; Gr: groundmass; s: secondary mineral.

**Table 3.** Lithological composition, key features and possible source regions of the three identified petrofacies discussed in the text.

**Figure Captions**

**Figure 1.** Bedmachine overview (Morlighem, 2019; Morlighem et al., 2020) of the Ross Sea region with sample site locations shown labeled as in Table 1 and simplified geologic map of the two sides of the Ross Sea Embayment. The position of the IODP Site U121, DSDP Site 270, ANDRILL, Cape Roberts Project (CRP), and CIROS cores is shown. Abbreviations are the following: ERS: Eastern Ross Sea; CRS: Central Ross Sea; WRS: Western Ross Sea; BIS: Bindschadler Ice Stream; BG: Beardmore Glacier; BY: Byrd Glacier; EP: Edward VII Peninsula; FR: Flood Range; KIS: Kamb Ice Stream; KG: Koettlitz Glacier; MG: Mulock Glacier; NG: Nimrod Glacier; OR: Ohio Range; QMM: Queen Maud Mountains; RG: Reedy Glacier; RI: Roosevelt Island; SC: Scott Glacier; SH: Shackleton Glacier; SK: Skelton Glacier; WIS: Whillans Ice Stream; WM: Whitmore Mountains; U1521 is the IODP Site U121; 270 is the DSDP Site 270. Geological map is simplified from Cox et al. (2023); position of inferred Cenozoic volcanic edifices is from van Wyck de Vries (2018).

**Figure 2.** Photomicrographs of representative intrusive and extrusive igneous clasts recovered from Central and Western Ross Sea cores. A) thin section 24: hbl-tonalite (XPL); B) thin section 107: dolerite (XPL); C) thin section 34: leucocratic syeno-granite (XPL); D) thin section 78: rhyolite (XPL); E) thin section 71: trachytic volcanite (XPL); F) thin section 36: rhyolite (XPL). Pl: Plagioclase; Qtz: Quartz; Or: Orthoclase; Cpx: clinopyroxene; Ep: Epidote; Krs: Kaersutite.

**Figure 3.** Photomicrographs of representative sedimentary and metamorphic clasts recovered from Central and Western Ross Sea cores; A) thin section 33: microsparitic mudstone (PPL); B) thin section 91: microsparitic limestone (XPL); C) thin section 81: sub-arkose (PPL); D) thin section 75: graywacke (PPL); E) thin section 25: biotite-white mica schist (XPL); F) thin section 27: biotite schist (XPL); G) thin section 92: medium grained foliated biotite meta-sandstone (XPL); H) thin section 94: marble (PPL); I) thin section 37: biotite-clinoamphibole phyllite (XPL). Cal: Calcite; Kfs: alkali feldspar; Qtz: Quartz; Mat: Matrix; Bt: Biotite; Wm: White mica; Pl: Plagioclase.

**Figure 4.** A: enlarged view of Ross Sea embayment taken from figure 1 showing position of analyzed cores and an ideal E-W section from Marie Byrd Land to Southern Victoria Land. B: relative occurrence and distribution of gravel sized clasts from each core along the E-W transect.

**Figure 5.** A) Discriminant analysis plot of the three considered petrofacies (PF); B) Box plot showing the values of the six lithological groups for the three petrofacies (PF).

**Figure 6.** Representative chemical analysis of minerals from Western and Central Ross Sea detrital clasts (Eastern Ross sea data are available in Perotti et al. 2017): (a) Ca-amphibole classification from Leake et al. (1997), in terms of $X_{Mg}$ versus Si (atoms per formula unit); triangles refer to amphiboles of the edenite-pargasite series ($Na+K_A \geq 0.50$ and $Ti>0.50$ atoms per formula unit, i.e. kaersutite field) (b) biotite composition in terms of $Al^{IV}$ versus $X_{Fe}$; (c)

white mica composition in terms of Al versus Si (top) and Fe+Mg versus Si (bottom, atoms per formula unit).

**Figure 7.** Petrofacies (PF) distribution in Eastern (ERS), Central (CRS) and Western (WRS) Ross Sea. Main features of the PF are discussed in the text and shown in Figure 5. Abbreviation and geological legend as in Figure 1. White-bounded symbols indicate the occurrence of carbonate clasts. Pink octagon is ELT27-14 site, that is the easternmost site involved in expansion of Byrd Glacier ice during the LGM in the model of Licht and Palmer (2013). Green rhombus is the westernmost site that yielded a zircon U/Pb population of age around 100 Ma, interpreted to be a diagnostic feature of West Antarctica provenance (Licht et al., 2014). Abbreviations as in figure 1. Dotted blue arrows show the indicative ice flow paths that best fit our clast data.

**Declaration of interests**

☒The authors declare that they have no known competing financial interests or personal relationships that could have appeared to influence the work reported in this paper.

☐The authors declare the following financial interests/personal relationships which may be considered as potential competing interests:

Table 1

| Area | Cruise | Core | Label | Lat. | Long. | Water depth (m) | Core length (cm) | Clasts count |
|---|---|---|---|---|---|---|---|---|
| Sulz.Bay | NBP96-01 | 011-PC | 96-11 | -76.78 | -155.44 | 392 | 389 | 259 |
| Sulz.Bay | NBP96-01 | 014-PC | 96-14 | -76.59 | -155.55 | 369 | 154 | 48 |
| Sulz.Bay | NBP96-01 | 016-PC | 96-16 | -76.91 | -155.93 | 1273 | 65 | 172 |
| ERS | NBP96-01 | 010-PC | 96-10 | -77.23 | -160.11 | 493 | 190 | 13 |
| ERS | NBP96-01 | 008-PC | 96-08 | -77.56 | -160.94 | 650 | 202 | 163 |
| ERS | NBP96-01 | 009-PC | 96-09 | -77.61 | -160.85 | 643 | 210 | 58 |
| ERS | ELT32 | 026-PC | 32-26 | -78.07 | -162.39 | 605 | 247 | 29 |
| ERS | ELT32 | 027-PC | 32-27 | -77.78 | -160.63 | 670 | 148 | 185 |
| ERS | NBP99-02 | 017-PC | 99-17 | -77.72 | -161.86 | 715 | 205 | 33 |
| ERS | DF83 | 014-PC | 83-14 | -78.48 | -164.14 | 601 | 277 | 40 |
| ERS | NBP94-07 | 056-PC | 94-56 | -77.33 | -166.66 | 441 | 362 | 60 |
| ERS | NBP94-07 | 057-PC | 94-57 | -77.34 | -167.36 | 525 | 89 | 23 |
| ERS | NBP94-07 | 058-PC | 94-58 | -77.35 | -167.46 | 525 | 315 | 53 |
| ERS | NBP94-07 | 061-PC | 94-61 | -77.23 | -168.04 | 548 | 36 | 8 |
| ERS | NBP94-07 | 063-PC | 94-63 | -77.33 | -169.18 | 582 | 292 | 53 |
| ERS | NBP94-07 | 065-PC | 94-65 | -77.47 | -168.44 | 587 | 116 | 13 |
| ERS | NBP99-02 | 004-PC | 99-4 | -78.15 | -168.58 | 618 | 104 | 18 |
| CRS | DF62-01 | 022-PC | 62-22 | -78.12 | -173.88 | 549 | 259 | 23 |
| CRS | DF76 | 003-PC | 76-3 | -78.2 | -174,183 | 558 | 671 | 49 |
| CRS | DF76 | 006-PC | 76-6 | -77.87 | -179.18 | 640 | 478 | 43 |
| CRS | DF76 | 008-PC | 76-8 | -77,533 | -175,933 | 576 | 351 | 24 |
| CRS | DF76 | 010-PC | 76-10 | -77.45 | -178.62 | 613 | 279 | 55 |
| CRS | DF78 | 012-PC | 78-12 | -78,267 | -175.25 | 538 | 271 | 35 |
| CRS | NBP93-08 | 013-PC | 93-13 | -77,369 | -177,987 | 676 | 217 | 42 |
| CRS | NBP94-01 | 036-PC | 94-36 | -75.82 | -177.22 | 622 | 96 | 5 |
| CRS | NBP94-07 | 043-PC | 94-43 | -77,917 | -178,822 | 725 | 241 | 27 |
| CRS | NBP94-07 | 45-PC | 94-45 | -77,633 | -179,391 | 661 | 172 | 11 |
| CRS | NBP94-07 | 049-PC | 94-49 | -77,534 | -177,775 | 670 | 316 | 40 |
| CRS | NBP94-07 | 090-PC | 94-90 | -76.76 | 178,535 | 298 | 359 | 107 |
| CRS | NBP95-01 | 011-PC | 95-11 | -76.45 | -179.09 | 659 | 165 | 22 |
| CRS | NBP95-01 | 017-PC | 95-17 | -77.45 | 179.05 | 732 | 202 | 20 |
| CRS | NBP96-01 | 002-JPC | 96-2 | -76,452 | 179,881 | 373 | 419 | 106 |
| CRS | NBP00-01 | 01-PC | 00-1 | -78.02 | -176.25 | 578 | 237 | 165 |
| WRS | DF78 | 009-PC | 78-9 | -76.97 | 167.87 | 437 | 158 | 13 |
| WRS | DF80 | 133-PC | 80-133 | -77,083 | 166,167 | 897 | 258 | 9 |
| WRS | DF80 | 189-PC | 80-189 | -77.2 | 167,883 | 907 | 193 | 34 |
| WRS | NBP94-01 | 002-PC | 94-2 | -76,284 | 169,704 | 679 | 174 | 36 |
| WRS | NBP94-01 | 016-PC | 94-16 | -74.65 | 174.57 | 465 | 390 | 33 |

| | | | | | | | | |
|---|---|---|---|---|---|---|---|---|
| WRS | NBP94-01 | 031-PC | 94-31 | -75.17 | 178.55 | 473 | 188 | 10 |
| WRS | NBP94-07 | 001-PC | 94-01 | -74.98 | 179.36 | 443 | 231 | 26 |
| WRS | NBP94-07 | 012-PC | 94-12 | -75.79 | 177.17 | 453 | 212 | 4 |
| WRS | ELT32 | 013-PC | 32-13 | -74.96 | 172.16 | 536 | 207 | 20 |

Table 2

| Area | Thin Section ID | Piston core label | Depth (cm) | Lithology | Pl (%) | Amp (%) | Bt (%) | Qtz (%) | Opm (%) | Kfs (%) | Cal (%) | Cpx (%) | Ol (%) | Grt (%) | Czo-Ep (%) | Ttn (%) | Ap (%) | Zrn (%) | Chl (%) | Wm (%) | Lit (%) | Mat (%) | Gr (%) | Glass (%) | Grain Size |
|---|---|---|---|---|---|---|---|---|---|---|---|---|---|---|---|---|---|---|---|---|---|---|---|---|---|
| CRS | 24 | 76-3 | 397-399 | foliated hbl-tonalite | 42 | 14 | 5 | 38 | 1 | | | | | | 2 | <1 | <1 | | s | s | | | | | fg-mg |
| CRS | 25 | 76-3 | 595-599 | bt-wm schist | 3 | | 12 | 75 | | | | | | | | | <1 | <1 | | 9 | | | | | fg |
| CRS | 26 | 94-49 | 13-14 | cam-bt schist | 2 | 20 | 7 | 66 | <1 | | 3 | | | | <1 | 1 | <1 | <1 | | | | | | | fg |
| CRS | 27 | 94-43 | 184-185 | bt-schist | 2 | | 25 | 71 | | | | | | | | | <1 | | | 1 | | | | | fg |
| CRS | 28 | 94-78 | 220-223 | dolerite | 67 | | | | 1 | | | 33 | | | | | | | | | | | | | mg |
| CRS | 29 | 94-78 | 210-213 | lithoarenite mylonitic | | | | 50 | | | 12 | | | | | | | | | | 29 | | | | mg-cg |
| CRS | 30 | 94-90 | 34-35 | monzogranite | 30 | | 4 | 40 | <1 | 24 | | | | | 1 | | | | s | | | | | | mg-cg |
| CRS | 31 | 94-90 | 112-113 | bt-hbl granodiorite | 35 | 9 | 6 | 45 | | 5 | | | | | | <1 | <1 | <1 | s | | | | | | fg-mg |
| CRS | 32 | 94-90 | 165-167 | bt-monzogranite | 47 | | | 25 | 1 | 20 | | | | | 1 | | <1 | | 7 | | | | | | mg |
| CRS | 33 | 78-12 | 83-85 | microsparitic mudstone | | | | <1 | 1 | | 98 | | | | | | | | | | | | | | vfg |
| CRS | 34 | 78-12 | 71-79 | leucocratic syeno-granite | 10 | | | 49 | <1 | 37 | | | | | <1 | | | | 3 | <1 | | | | | cg |
| CRS | 35 | 78-12 | 136-137 | bt-wm-schist | | | 10 | 84 | | 2 | | | | <1 | | | <1 | | 3 | | | | | | fg |

| | | | | | | | | | | | | | | | | | | | | | | |
|---|---|---|---|---|---|---|---|---|---|---|---|---|---|---|---|---|---|---|---|---|---|---|
| C | | 78 | | | | | | | | | | | | | | | | | | | | |
| R | | - | 85- | | | | | | | | | | | | | | | | | | 8 | m |
| S | 78 | 12 | 87 | rhyolite | 6 | | | 9 | | 2 | | | | | | | | | | | 3 | g |
| C | | 94 | | | | | | | | | | | | | | | | | | | | fg- |
| R | | - | 93- | metasand | | | | 9 | | | | | | | | < | < | | | | | m |
| S | 79 | 43 | 97 | stone | 1 | | 3 | 2 | | 1 | | | | 1 | | 1 | 1 | | 1 | | | g |
| C | | 94 | | | | | | | | | | | | | | | | | | | | |
| R | | - | | wm- | | | | 9 | | | | | | | | < | | | | | | |
| S | 80 | 43 | 4-7 | quartzite | | | | 5 | 1 | | | | | | | 1 | | | 3 | | | fg |
| C | | 94 | 107 | | | | | | | | | | | | | | | | | | | m |
| R | | - | - | sub- | | | | 8 | < | | | | | | | | | | < | | | g- |
| S | 81 | 49 | 108 | arkose | 2 | | 3 | 7 | 1 | 5 | 1 | | | | | | | | 1 | 1 | | cg |
| C | | 94 | 275 | | | | | | | | | | | | | | | | | | | |
| R | | - | - | | | | 1 | 8 | < | | | | | | | < | | | < | | | |
| S | 82 | 49 | 276 | bt-schist | 1 | | 2 | 6 | 1 | | | | | | | 1 | | | 1 | | | fg |
| C | | 94 | 262 | | | | | | | | | | | | | | | | | | | |
| R | | - | - | bt-wm | | | 2 | 7 | | | | | | | | < | | | | | | |
| S | 83 | 55 | 264 | schist | 2 | | 1 | 4 | | | | | | | | 1 | | | 2 | | | fg |
| C | | 94 | 220 | | | | | | | | | | | | | | | | | | | |
| R | | - | - | | 6 | | | < | | | | 3 | | | | | | | | | | m |
| S | 84 | 78 | 221 | Gabbro | 2 | | | 1 | 2 | | | 5 | | | | | | | | | | g |
| C | | 94 | | | | | | | | | | | | | | | | | | | | |
| R | | - | 92- | metasand | | < | 1 | 6 | | | | | | | | < | < | | | | | |
| S | 85 | 90 | 93 | stone | 3 | 1 | 9 | 6 | | | 2 | | | 8 | 1 | 1 | 1 | | | | | fg |
| C | | | | foliated | | | | | | | | | | | | | | | | | | m |
| R | | 76 | 86- | Bt- | 3 | | 1 | 4 | < | | | | | | | < | < | | | | | g- |
| S | 86 | -8 | 89 | tonalite | 5 | | 8 | 0 | 1 | 5 | | | | | | 1 | 1 | | | | | cg |
| C | | | | bt-wm | | | | | | | | | | | | | | | | | | |
| R | | 76 | 30- | schist | | | | | | | | | | | | | | | | | | |
| S | 87 | -8 | 35 | (altered) | | | | | | | | | | | | | | | | | | fg |
| C | | | 20. | | | | | | | | | | | | | | | | | | | |
| R | | 93 | 5- | bt-cam- | 2 | 1 | 1 | 4 | | | | | | | | < | < | | | | | m |
| S | 88 | -7 | 21 | gneiss | 5 | 5 | 2 | 5 | | | | | | | 1 | 1 | 1 | | | | | g |
| C | | | | | | | | | | | | | | | | | | | | | | fg- |
| R | | 93 | 53- | | | | 2 | N | < | | | | | | | | | | N | | | vf |
| S | 89 | -7 | 54 | Phyllite | | | 5 | D | 1 | | | | | | | | | | D | | | g |
| C | | | 122 | | | | | | | | | | | | | | | | | | | |
| R | | 93 | - | | | | 1 | 7 | < | | | | | | | < | < | | | | | |
| S | 90 | -7 | 123 | bt-schist | 3 | | 8 | 7 | 1 | | | | | | 1 | 1 | 1 | | | | | fg |
| C | | 93 | | | | | | | | | | | | | | | | | | | | |
| R | | - | 51- | | | | | | | | 9 | | | | | | | | | | | |
| S | 91 | 13 | 52 | limestone | | | | | 2 | | 8 | | | | | | | | | | | fg |
| C | | 93 | 133 | | | | | | | | | | | | | | | | | | | fg- |
| R | | - | - | metasand | | | 1 | 7 | | | | | | | | < | < | | | | | m |
| S | 92 | 13 | 134 | stone | 3 | | 2 | 7 | 1 | | 2 | | | | | 1 | 1 | | 4 | | | g |
| C | | 93 | 210 | | | | | | | | | | | | | | | | | | | |
| R | | - | - | | 5 | | | | | | | 3 | | | | | | | | | | |
| S | 93 | 13 | 211 | gabbro | 5 | | | 3 | 2 | | | 8 | | | | | | | | | | |
| C | | 93 | 216 | | | | | | | | | | | | | | | | | | | |
| R | | - | - | | | | | | | | 9 | | | | | | | | | | | m |
| S | 94 | 13 | 217 | marble | | | | | 1 | | 9 | | | | | | | | | | | g |
| C | | | 130 | | | | | | | | | | | | | | | | | | | fg- |
| R | | 96 | - | metasand | | | | 8 | | | | | | < | | < | | | | | | m |
| S | 95 | -2 | 135 | stone | 2 | | 8 | 4 | | 1 | 2 | | | 1 | | 1 | | | 2 | 1 | | g |
| C | | | 176 | | | | | | | | | | | | | | | | | | | |
| R | | 96 | - | meta- | N | | 5 | N | | | | | | | | | | | | | | |
| S | 96 | -2 | 177 | siltstone | D | | 5 | D | 1 | | | | | | | | | | 1 | | | fg |
| C | | | 249 | | | | | | | | | | | | | | | | | | | m |
| R | | 96 | - | | | | | 9 | | | | | | | | | < | | | | | g- |
| S | 97 | -2 | 250 | quartzite | 2 | | | 4 | | | | | | | | | 1 | 1 | 2 | | | cg |
| C | | 94 | 78- | bt- | | | 3 | 5 | | | | | | | | | | | | | | fg- |
| R | 98 | - | 79 | hornfels | 2 | | 8 | 7 | 1 | | | | | | | | | | 2 | | | m |

| | | | | | | | | | | | | | | | | | | | | | | |
|---|---|---|---|---|---|---|---|---|---|---|---|---|---|---|---|---|---|---|---|---|---|---|
| S | | 79 | | | | | | | | | | | | | | | | | | | | g |
| C | | 94 | | gneissic | | | | | | | | | | | | | | | | | | |
| R | | - | | calc- | | | | | | | | | | | | | | | | | | |
| S | 99 | 73 | 2-8 | schist | | | | | | | | | | | | | | | | | | |
| C | | 94 | 307 | | | | | | | | | | | | | | | | | | | |
| R | 10 | - | - | metasand | | | 4 | 4 | | | | | | | < | | | | | | | |
| S | 0 | 49 | 309 | stone | 1 | 3 | 5 | 7 | 1 | | 2 | | | | 1 | | | | | | | fg |
| C | | | | | | | | | | | | | | | | | | | | | | m |
| R | 10 | 94 | | gabbro/d | 6 | | | | | | | 3 | | | | | | | | | | g/ |
| S | 1 | -8 | 7-9 | olerite | 5 | | | 1 | 2 | | | 2 | | | | | | | | | | cg |
| C | | | 116 | | | | | | | | | | | | | | | | | | | |
| R | 10 | 94 | - | cam | | | 4 | 4 | < | | | | | | | | | | | | | |
| S | 2 | -8 | 119 | phyllite | | 9 | 4 | 5 | 1 | | | | | | | | | | | | | fg |
| C | | 94 | | bt- | | | | | | | | | | | | | | | | | | |
| R | 10 | - | 30- | metasand | | | 1 | 6 | | | | | | | | | | | 2 | | | m |
| S | 3 | 45 | 31 | stone | 2 | | 5 | 1 | | | | | | | | | | 2 | 0 | | | g |
| C | | 94 | 133 | bt meta- | | | | | | | | | | | | | | | | | | |
| R | 10 | - | - | sandston | | | 2 | 6 | | | 1 | | | | < | < | | | | | | |
| S | 4 | 45 | 135 | e | 1 | | 0 | 6 | 2 | | 0 | | | | 1 | 1 | | | | | | fg |
| C | | 94 | 237 | | | | | | | | | | | | | | | | | | | |
| R | 10 | - | - | | 4 | | 1 | 3 | | | | | | | < | < | | | | | | |
| S | 6 | 90 | 239 | bt-schist | 8 | | 5 | 5 | | | | | | | 1 | 1 | | 1 | | | | fg |
| C | | | 205 | | | | | | | | | | | | | | | | | | | |
| R | 10 | 96 | - | gabbro/d | 4 | | | | | | | 3 | | | | | | | | | | m |
| S | 7 | -2 | 206 | olerite | 3 | | | 1 | 1 | | | 5 | | | | | | | | | | g |
| | | 80 | | | | | | | | | | | | | | | | | | | | vf |
| W | | - | 168 | | | | | | | | | | | | | | | | | | | g- |
| R | | 18 | - | (meta) | N | | | 1 | | | | | | < | | < | | < | | 8 | | m |
| S | 36 | 9 | 169 | rhyolite | D | | | 5 | | | | | | 1 | | 1 | | 1 | 4 | 0 | | g |
| | | 80 | | | | | | | | | | | | | | | | | | | | |
| W | | - | 181 | | | | | | | | | | | | | | | | | | | |
| R | | 18 | - | cam bt | | | 3 | N | | | 1 | | | | | | | | | | | vf |
| S | 37 | 9 | 184 | phyllite | | 8 | 0 | D | | | 2 | | | | | | | | | | | g |
| W | | 78 | 125 | | | | | | | | | | | | | | | | | | | |
| R | | - | - | | | | 2 | 5 | | | | | | | < | < | | | | | | |
| S | 38 | 14 | 128 | bt-schist | 1 | | 5 | 4 | 2 | 7 | | | | | 1 | 1 | | | | | | fg |
| W | | 78 | 145 | | | | | | | | | | | | | | | | | | | fg- |
| R | | - | - | meta- | 1 | N | | 1 | | | | | | N | | | N | | | 7 | | m |
| S | 39 | 14 | 151 | porphyry | 0 | D | | 8 | | | | | | D | | | D | | | 0 | | g |
| W | | 78 | 290 | | | | | | | | | | | | | | | | | | | m |
| R | | - | - | | 4 | | | | | | | 5 | | | | | | | | | | g- |
| S | 40 | 14 | 294 | dolerite | 1 | | | 1 | 2 | 1 | | 5 | | | | | | | | | | cg |
| W | | | 117 | | | | | | | | | | | | | | | | | | | |
| R | | 94 | - | bt-cam | | | 1 | 6 | | | | | | | < | < | | | | | | |
| S | 41 | -2 | 121 | schist | 3 | 8 | 5 | 6 | | | | 5 | | 3 | 1 | 1 | | | | | | fg |
| W | | 32 | | | | | | | | | | | | | | | | | | | | |
| R | | - | 45- | | 6 | | | | | | | 3 | | | | | | | | | | |
| S | 70 | 13 | 46 | dolerite | 4 | | | 2 | 2 | | | 2 | | | | | | | | | | fg |
| W | | 32 | 112 | intermedi | | | | | | | | | | | | | | | | | | fg- |
| R | | - | - | ate | 2 | | | | | | | | | | | | | | | | 6 | m |
| S | 71 | 13 | 115 | volcanite | 5 | 4 | | | 2 | | | 4 | | | | | | | | | 5 | g |
| | | 80 | | | | | | | | | | | | | | | | | | | | |
| W | | - | 167 | | | | | | | | | | | | | | | | | | | |
| R | | 13 | - | metasand | | | 3 | 5 | | | | | | | < | | | | | | | |
| S | 72 | 3 | 169 | stone | | | 8 | 5 | | | 3 | | | | 1 | | | | | | | fg |
| W | | 95 | | | | | | | | | | | | | | | | | | | | fg- |
| R | | - | 73- | | 1 | | | 6 | < | | | | | | < | < | 1 | | | | | m |
| S | 73 | 25 | 80 | Chl-schist | 9 | | | 1 | 1 | | | | | | 1 | 1 | 5 | 2 | | | | g |
| W | | 80 | 144 | | | | | | | | | | | | | | | | | | | fg- |
| R | | - | - | | 2 | | | | | | | | | | | | | | | 6 | < | m |
| S | 74 | 13 | 147 | basalt | 9 | | | | | | | 8 | 3 | | | | | | | 0 | 5 | g |

| | | | | | | | | | | | | | | | | | | | |
|---|---|---|---|---|---|---|---|---|---|---|---|---|---|---|---|---|---|---|---|
| W | | 4 78 | 152 | | | | 7 | | | | < | < | < | < | | 1 | | | fg- |
| R | | - | - | graywack | | | | | | | | | | | | | | | m |
| S | 75 | 14 | 153 | e | 3 | | 9 | | | | 1 | 1 | 1 | 1 | 5 | 2 | | | g |
| | | | 216 | | | | | | | | | | | | | | | | |
| W | | 78 | - | | | | | | | | | | | | | | | | |
| R | | - | 217 | | | | 2 | | | | | | | | | | 8 | | vf |
| S | 76 | 14 | .5 | siltstone | | | 0 | | | | | | | | | | 0 | | g |
| W | | | 114 | | | | | | | | | | | | | | | | |
| R | | 94 | - | metasand | | 1 | 7 | < | | | | < | | | | | | | |
| S | 77 | -2 | 118 | stone | 2 | 5 | 9 | 1 | | | | 1 | | 1 | 2 | | | | fg |

Table 3

| Petrofacies | Main lithologies | Key features | Possible source regions |
|---|---|---|---|
| PF A | phyllite, meta-sandstone, biotite ± white mica schist, quartzite, biotite ± hornblende granodiorite to tonalite, basat, felsic volcanic rocks | Metamorphic clasts > 55% Volcanic clasts < 20% | Transtantarctic Mountains<br>Marie Byrd Land<br>mixed source |
| PF A | phyllite, meta-sandstone, biotite ± white mica schist, quartzite, biotite ± hornblende granodiorite to tonalite, basat, felsic volcanic rocks | Metamorphic clasts > 55% Volcanic clasts < 20% carbonate clasts occur | Transtantarctic Mountains - Byrd-Beardmore glaciers |
| PF B | basalt, phyllite, meta-sandstone, biotite ± white mica schist, quartzite, biotite ± hornblende granodiorite to tonalite | Volcanic clasts > 20% | Transtantarctic Mountains - southern Victoria Land |
| PF C | biotite ± hornblende granodiorite to tonalite, phyllite, meta-sandstone, biotite ± white mica schist, quartzite, basat, felsic volcanic rocks | Granitoid clasts > 30% | Transtantarctic Mountains<br>Marie Byrd Land |
| PF C | biotite ± hornblende granodiorite to tonalite, phyllite, meta-sandstone, biotite ± white mica schist, quartzite, basat, felsic volcanic rocks | Granitoid clasts > 30% carbonate clasts occur | Transtantarctic Mountains - Byrd-Beardmore glaciers |

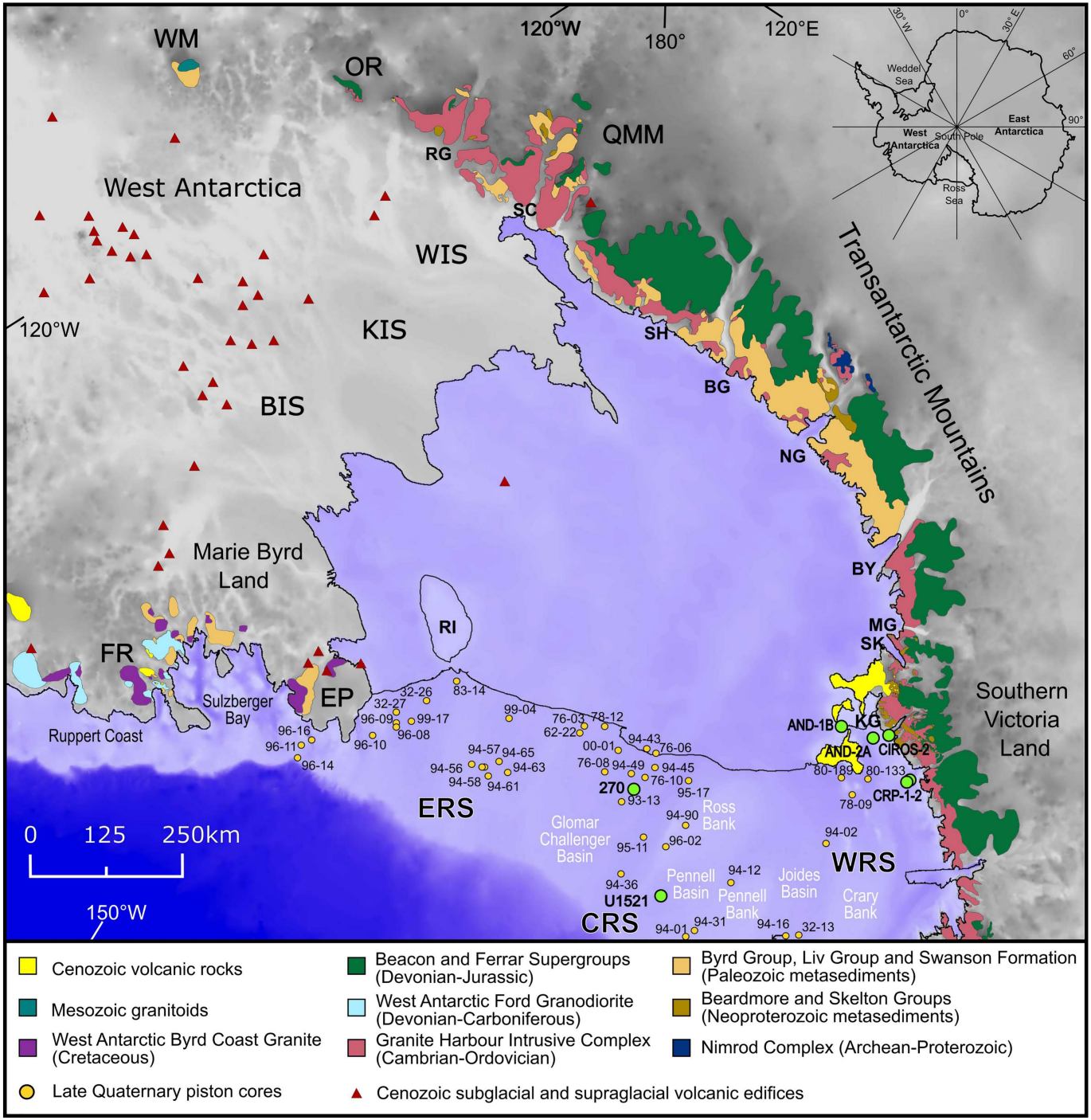
WM
OR
120°W
180°
120°E
QMM
RG
SC
West Antarctica
WIS
KIS
120°W
BIS
SH
BG
NG
Transantarctic Mountains
BY
MG
SK
Marie Byrd Land
RI
FR
EP
Sulzberger Bay
Ruppert Coast
ERS
Glomar Challenger Basin
Ross Bank
Pennell Basin
Pennell Bank
Joides Basin
Crary Bank
WRS
CRS
U1521
270
AND-1B
KG
AND-2A
CIROS-2
CRP-1-2
Southern Victoria Land
0 125 250km
150°W
Weddel Sea
West Antarctica
East Antarctica
South Pole
Ross Sea
30°W
0°
30°E
60°
90°
Cenozoic volcanic rocks
Mesozoic granitoids
West Antarctic Byrd Coast Granite (Cretaceous)
Late Quaternary piston cores
Beacon and Ferrar Supergroups (Devonian-Jurassic)
West Antarctic Ford Granodiorite (Devonian-Carboniferous)
Granite Harbour Intrusive Complex (Cambrian-Ordovician)
Cenozoic subglacial and supraglacial volcanic edifices
Byrd Group, Liv Group and Swanson Formation (Paleozoic metasediments)
Beardmore and Skelton Groups (Neoproterozoic metasediments)
Nimrod Complex (Archean-Proterozoic)

Figure 1

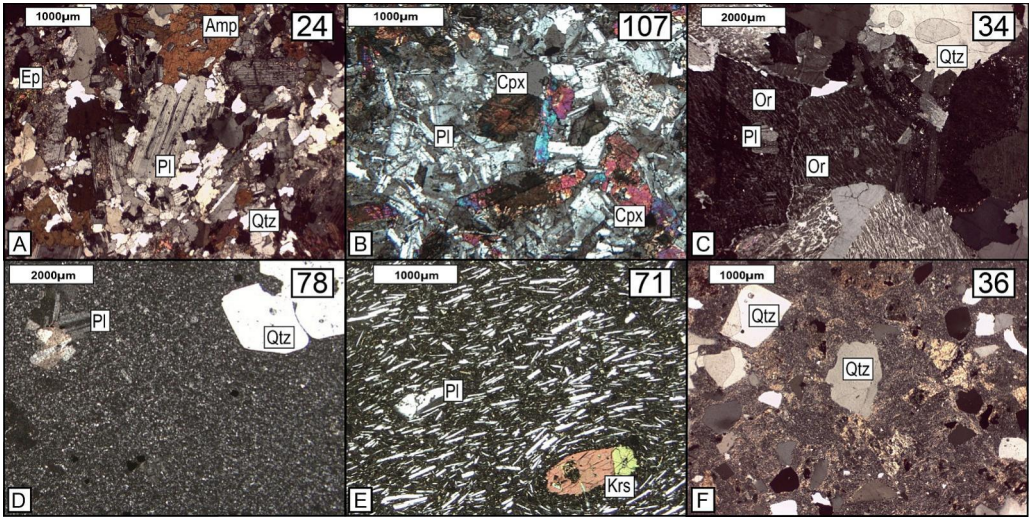
1000µm
Amp
24
Ep
Pl
Qtz
A
1000µm
107
Cpx
Pl
Cpx
B
2000µm
34
Qtz
Or
Pl
Or
C
2000µm
78
Pl
Qtz
D
1000µm
71
Pl
Krs
E
1000µm
36
Qtz
Qtz
F

Figure 2

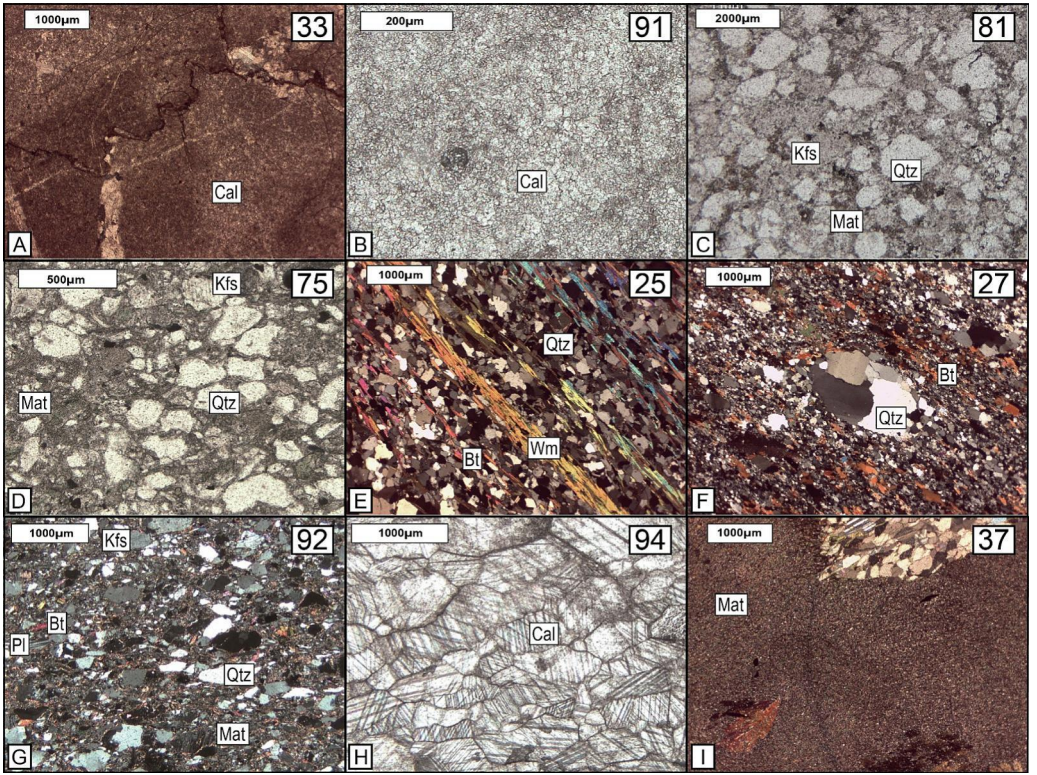
1000µm
33
Cal
A
200µm
91
Cal
B
2000µm
81
Kfs
Qtz
Mat
C
500µm
Kfs
75
Mat
Qtz
D
1000µm
25
Qtz
Wm
Bt
E
1000µm
27
Bt
Qtz
F
1000µm
Kfs
92
Bt
Pl
Qtz
Mat
G
1000µm
94
Cal
H
1000µm
37
Mat
I

Figure 3

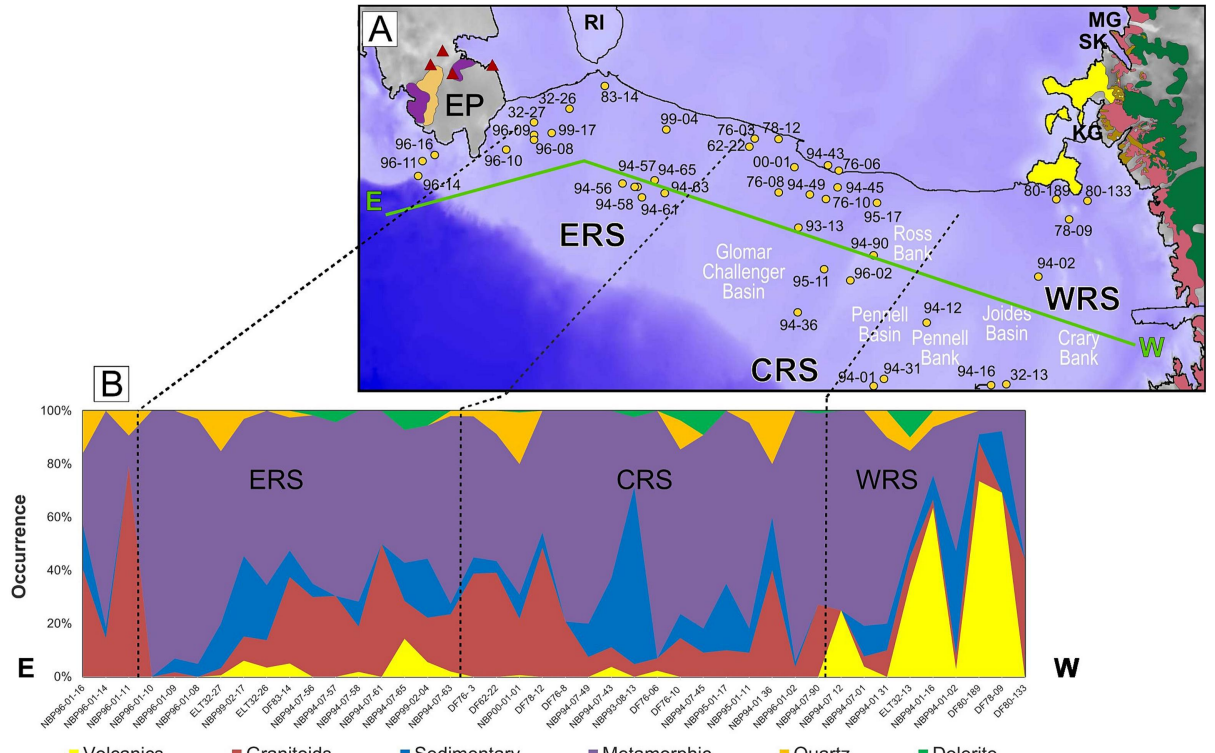
A
RI
MG
SK
KG
EP
32-26
83-14
32-27
99-04
99-17
96-09
76-03
78-12
96-16
96-08
62-22
96-11
96-10
00-01
94-43
96-06
96-14
94-57
94-65
94-56
94-63
76-08
94-49
94-45
80-89
80-133
E
94-58
94-61
76-10
94-13
95-17
78-09
ERS
Ross
Bank
94-90
Glomar
Challenger
Basin
94-02
95-11
96-02
WRS
94-12
Pennell
Basin
Joides
Basin
94-36
Pennell
Bank
Crary
Bank
W
CRS
94-01
94-31
94-16
32-13
B
100%
80%
60%
40%
20%
0%
Occurrence
ERS
CRS
WRS
E
W
NBP96-01-16
NBP96-01-14
NBP96-01-11
NBP96-01-10
NBP96-01-09
NBP96-01-08
ELT32-27
NBP99-02-17
ELT32-26
DF83-14
NBP94-07-56
NBP94-07-57
NBP94-07-58
NBP94-07-61
NBP94-07-65
NBP99-02-04
NBP94-07-63
DF76--3
DF82-22
NBP00-01-01
DF78-12
DF76-8
NBP94-07-49
NBP94-07-43
NBP93-08-13
DF76-06
DF76-10
NBP94-07-45
NBP95-01-17
NBP94-01-36
NBP95-01-11
NBP96-01-02
NBP94-07-90
NBP94-07-12
NBP94-07-01
NBP94-01-31
ELT32-13
NBP94-01-16
NBP94-01-02
DF80-189
DF78-09
DF80-133
Volcanics
Granitoids
Sedimentary
Metamorphic
Quartz
Dolerite

Figure 4

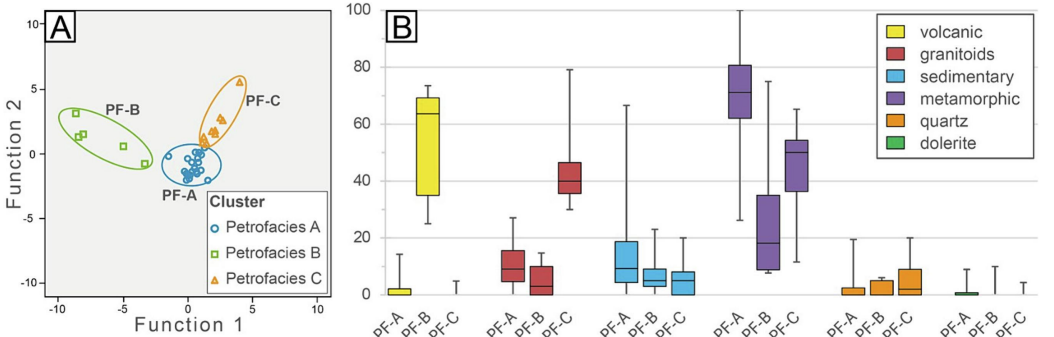
A
PF-B
PF-C
PF-A
Cluster
Petrofacies A
Petrofacies B
Petrofacies C
Function 2
Function 1
B
volcanic
granitoids
sedimentary
metamorphic
quartz
dolerite
PF-A
PF-B
PF-C

Figure 5

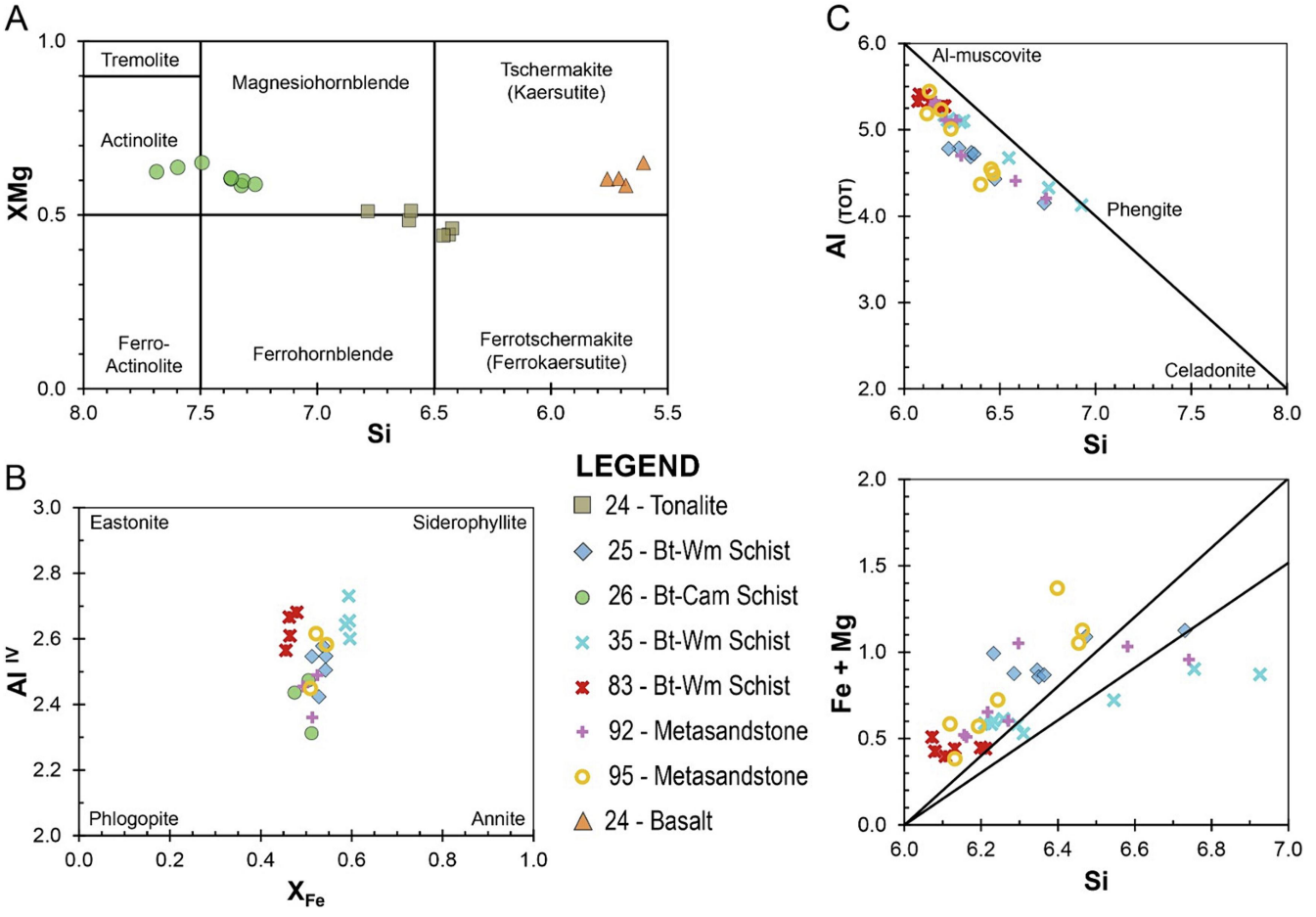
A
Tremolite
Magnesiohornblende
Tschermakite
(Kaersutite)
Actinolite
Ferro-
Actinolite
Ferrohornblende
Ferrotschermakite
(Ferrokaersutite)
XMg
Si
B
Eastonite
Siderophyllite
Phlogopite
Annite
Al IV
X Fe
LEGEND
24 - Tonalite
25 - Bt-Wm Schist
26 - Bt-Cam Schist
35 - Bt-Wm Schist
83 - Bt-Wm Schist
92 - Metasandstone
95 - Metasandstone
24 - Basalt
C
Al-muscovite
Phengite
Celadonite
Al (TOT)
Si
Fe + Mg
Si

Figure 6

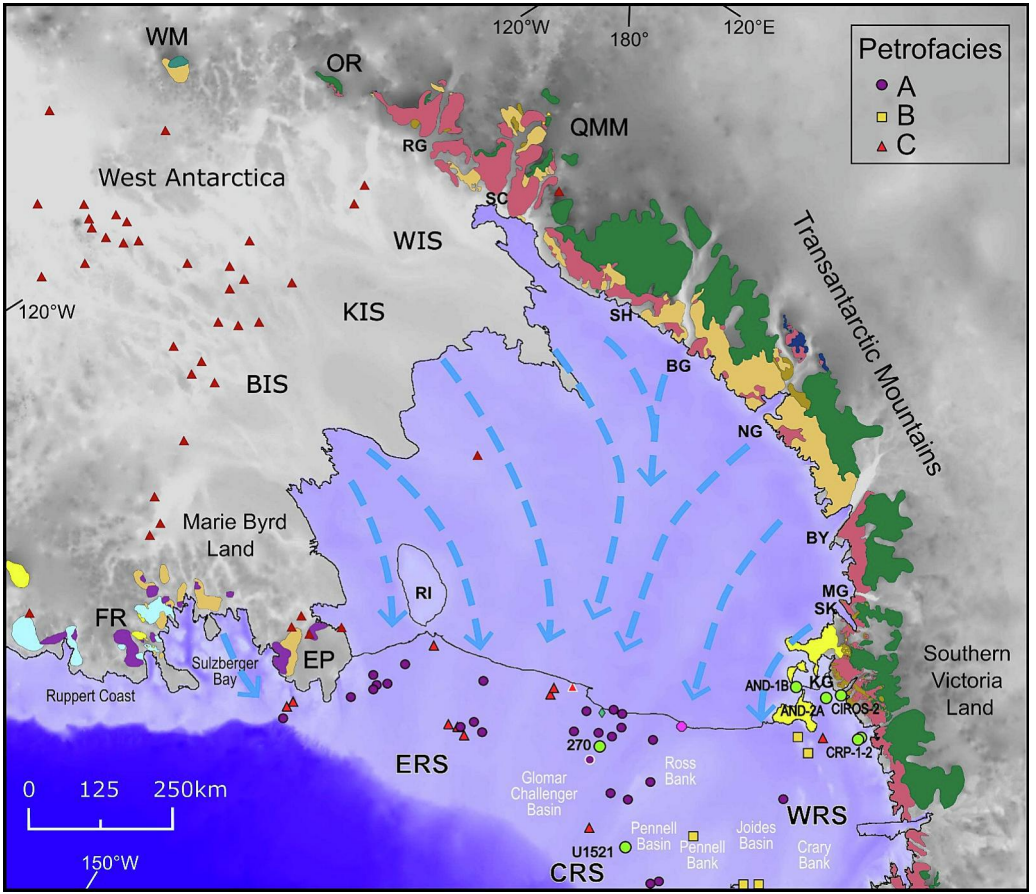
WM
OR
120°W
180°
120°E
Petrofacies
A
B
C
QMM
RG
West Antarctica
SC
WIS
Transantarctic Mountains
120°W
KIS
SH
BG
BIS
NG
Marie Byrd Land
BY
RI
MG
SK
FR
Sulzberger Bay
EP
Ruppert Coast
Southern Victoria Land
AND-1B
KG
AND-2A
CIROS-2
270
CRP-1-2
ERS
Ross Bank
Glomar Challenger Basin
0 125 250km
WRS
Pennell Basin
Joides Basin
Pennell Bank
Crary Bank
U1521
CRS
150°W

Figure 7